Terrain-Induced Asymmetric Structures of Typhoon Nari (2001)

Ming-Jen Yang 楊明仁

Dept. of Atmospheric Sciences, Inst. of Hydrological & Oceanic Sciences

National Central University

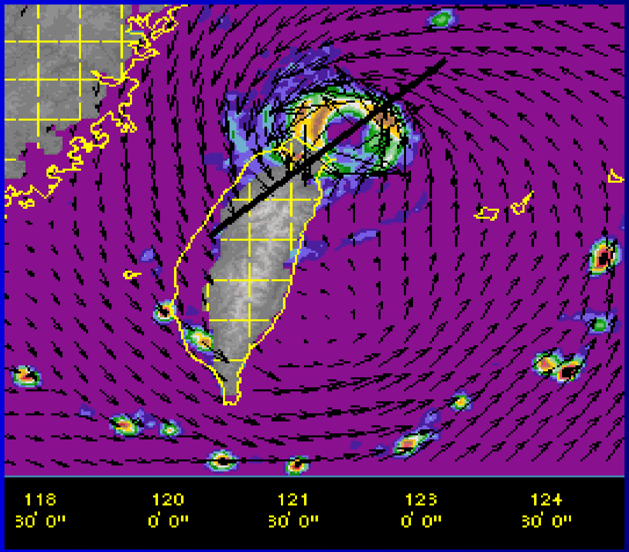

Collaborator: Da-Lin Zhang, Chi-Hsin Liao, and Xiao-Dong Tang

Seminar at NTU, 2009/10/06

Objectives

- 1) To document the evolution of Nari's precipitation, kinematic, and microphysics structures during its landfall on Taiwan
- 2) To investigate the terrain-induced asymmetric structures of Nari
- 3) To examine the physical mechanism responsible of the sloping mid-level radial outflow over the topography

Track Comparison

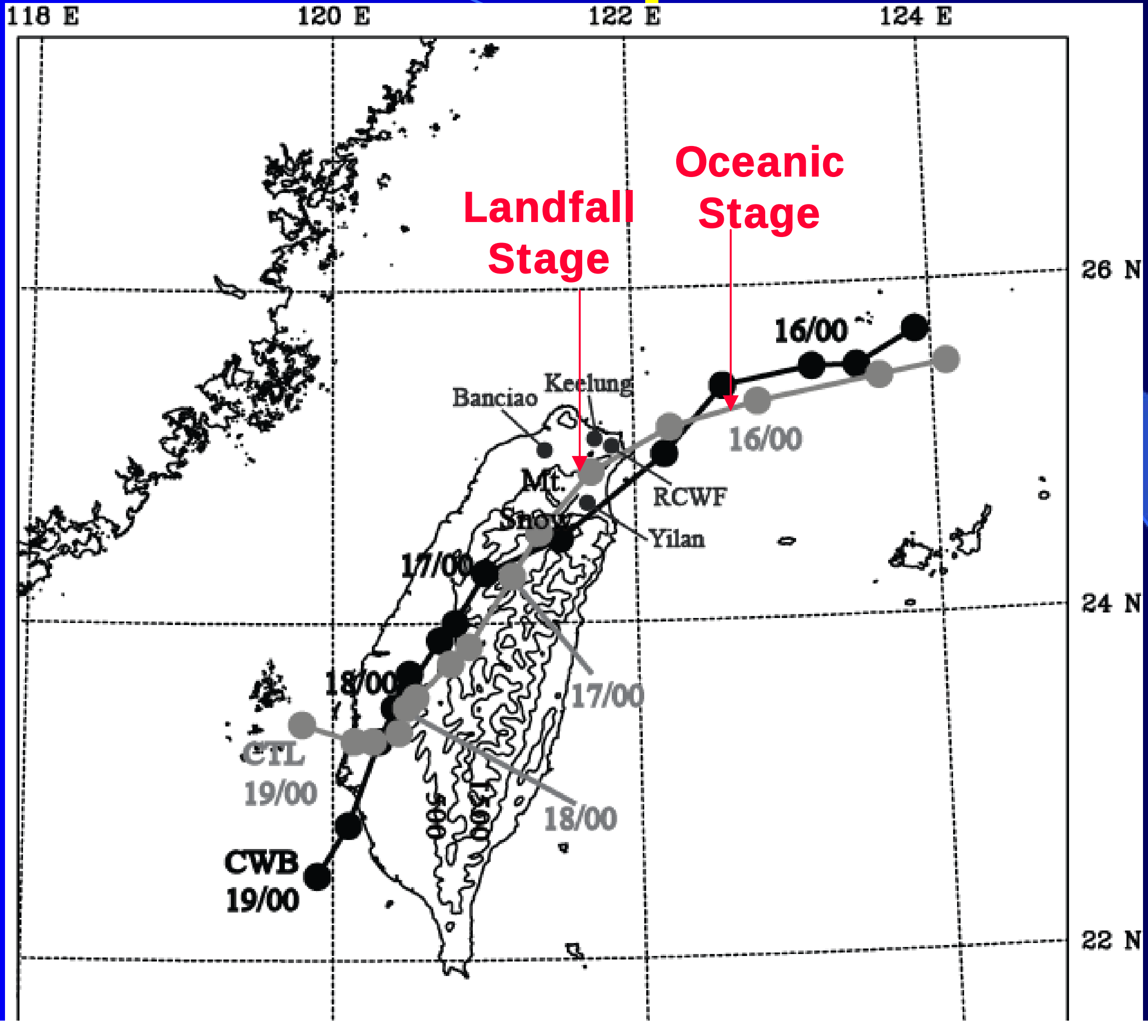

Yang et al. (2008; JAS)

Simulation time (hr)	12	24	36	48	60	72	84
Track error (km)	43.3	61.2	26.8	13.4	12	8.5	104.8

Time Series of SLP and Vmax

Yang et al. (2008; JAS)

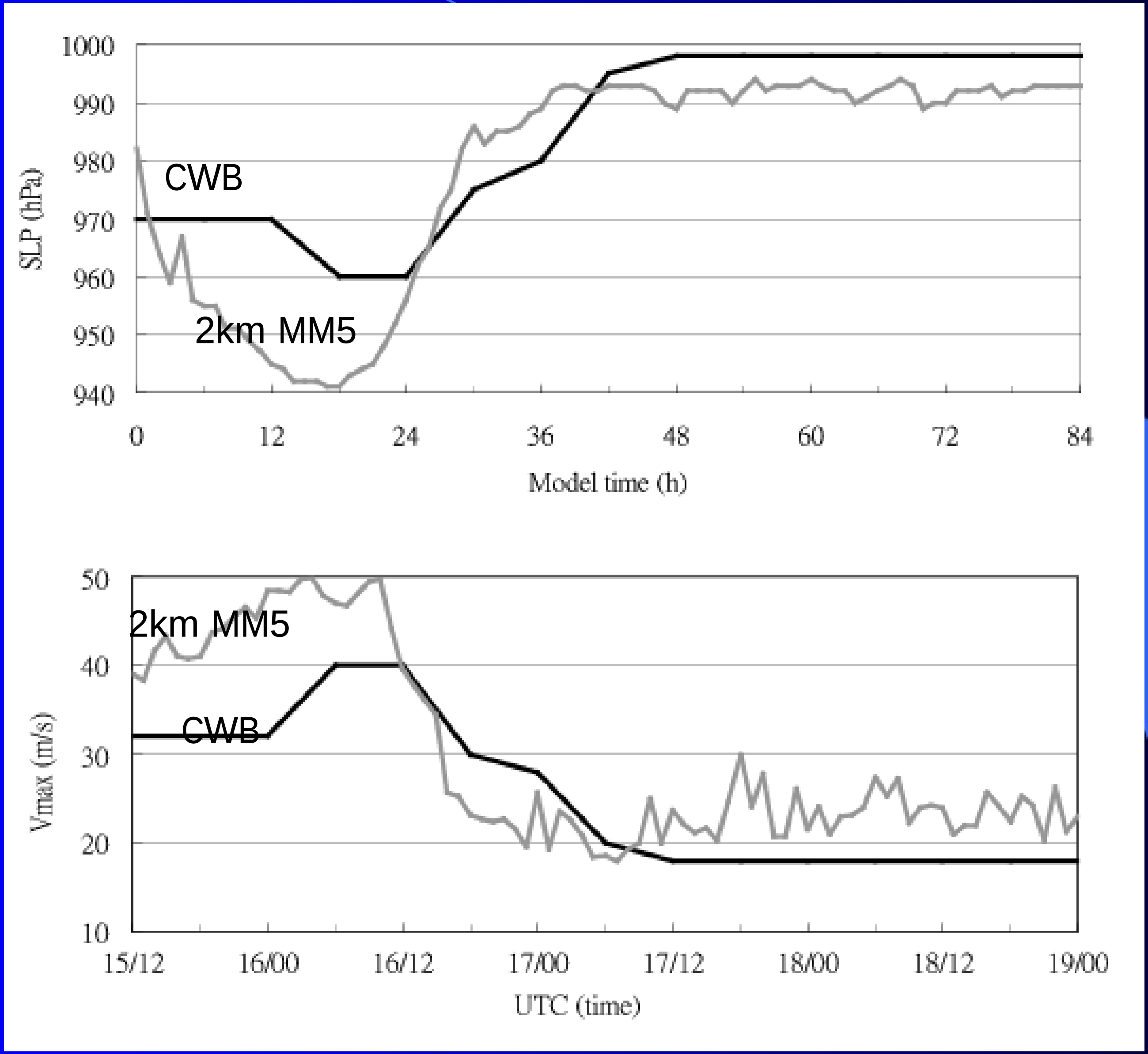

Horizontal Cross Section of Pressure Perturbations

0916_1400 UTC

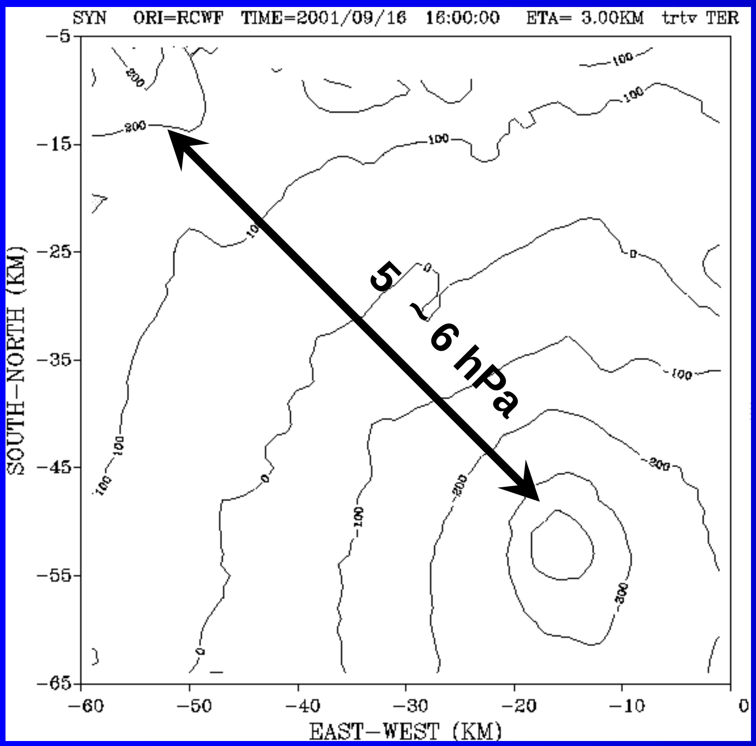

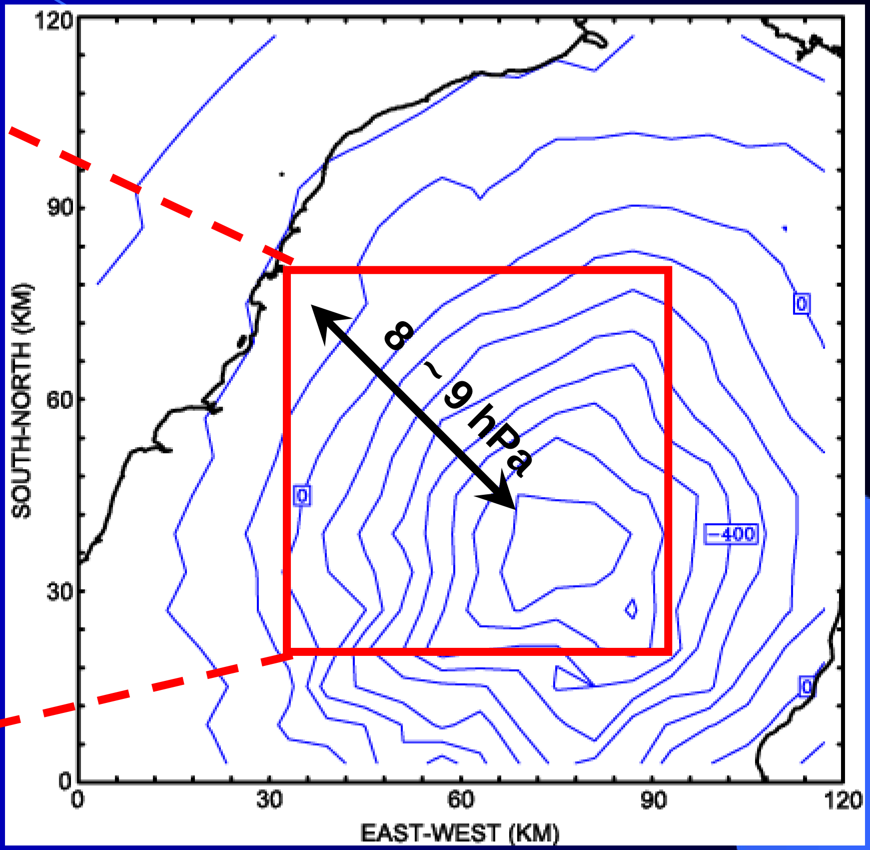

Radar Retrieval (wrt. a Station Sounding)

MM5 Simulation (wrt. a Horizontal Area Mean)

Courtesy of T.-C. Chen and Y.-C. Liou

Radial Wind wrt RCWF Radar
@ 3 km Height

Obs Vr (6 km pixel)

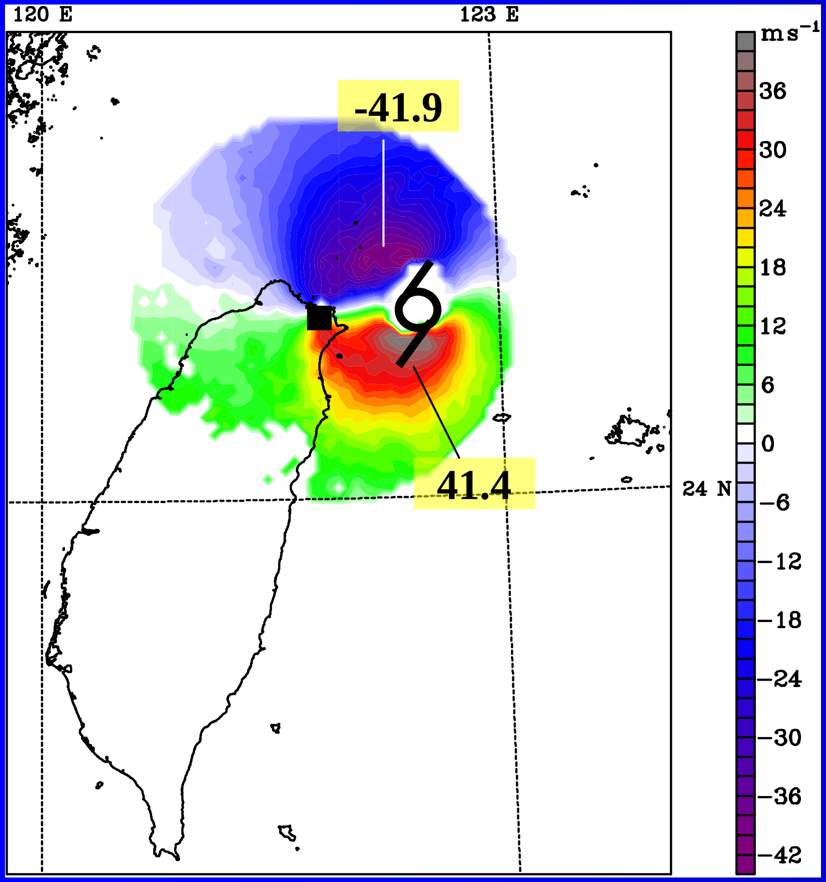

MM5 Vr (dx = 6 km)

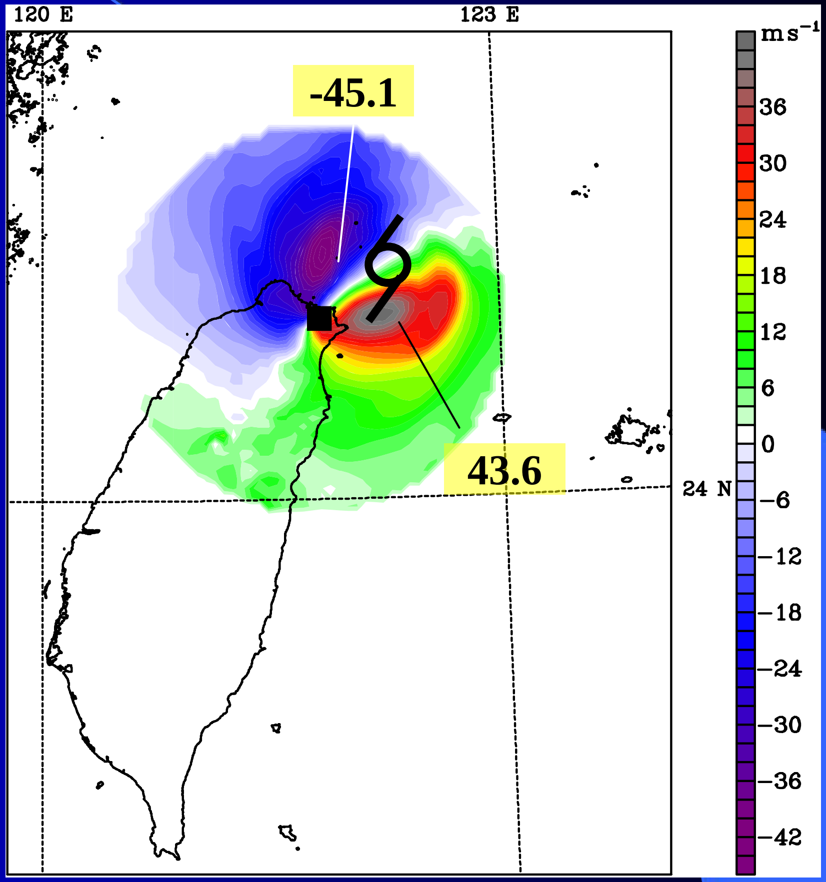

Courtesy of T.-C. Chen and Y.-C. Liou

3-day rainfall (09/16~09/18)

OBS 6km MM5 2km MM5

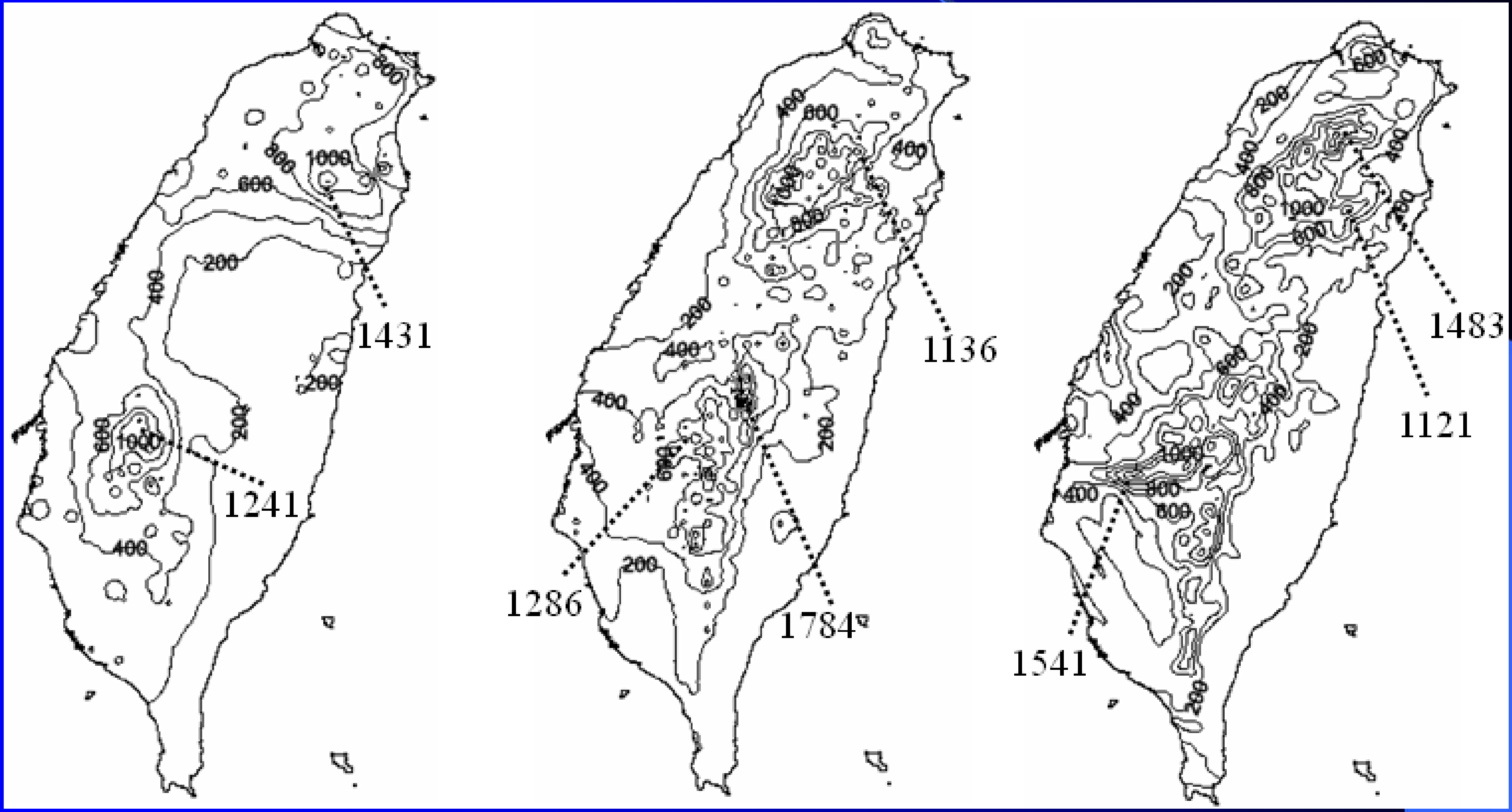

Oceanic Stage
(9 Hours Before Landfall)

Azimuthal-avg. structure (r=200 km) while Nari is over ocean

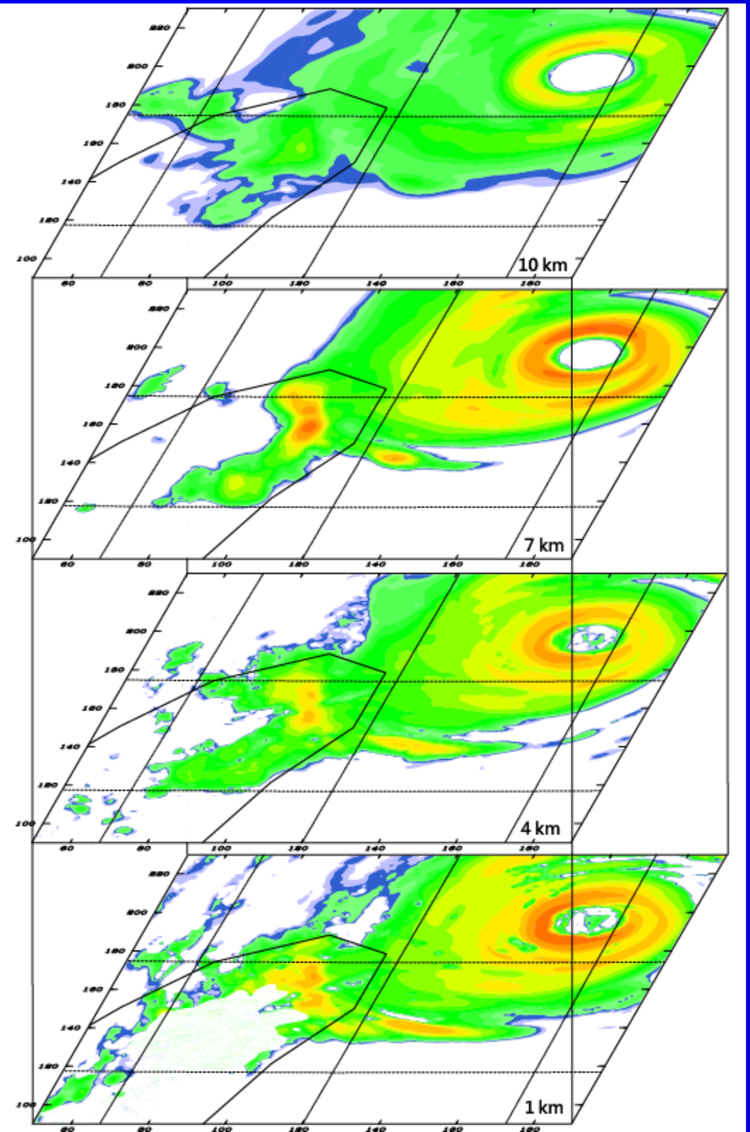

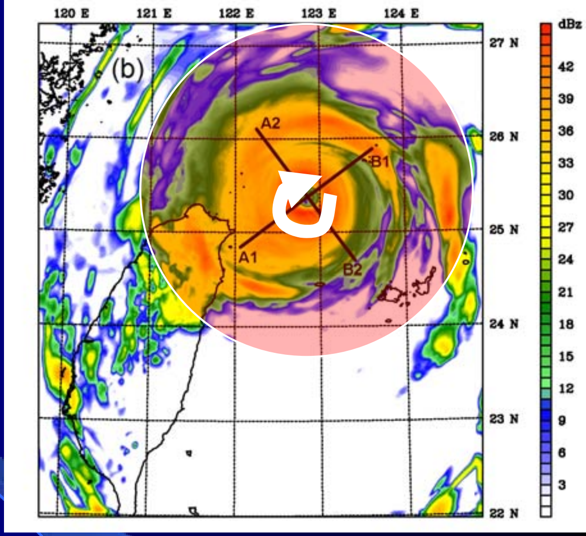

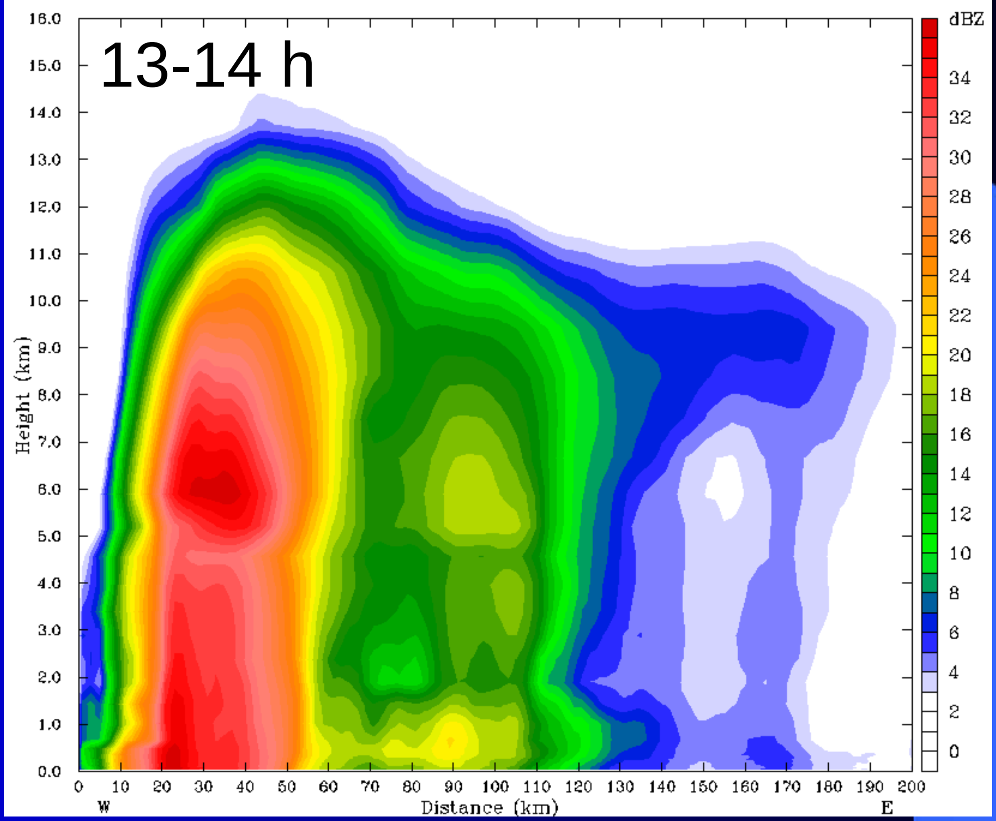

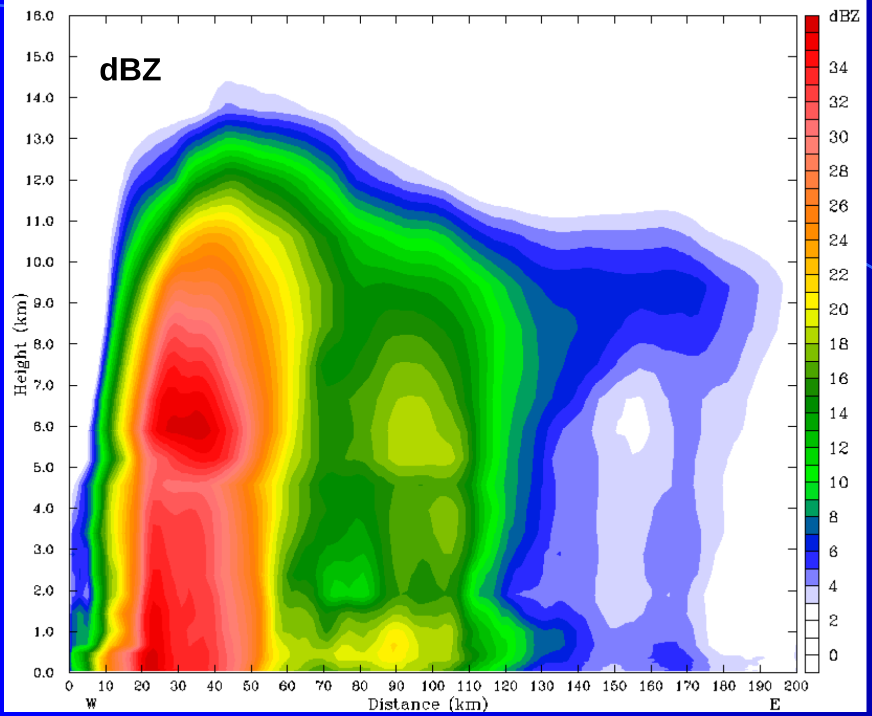
dBZ
Height (km)
Distance (km)
W
E

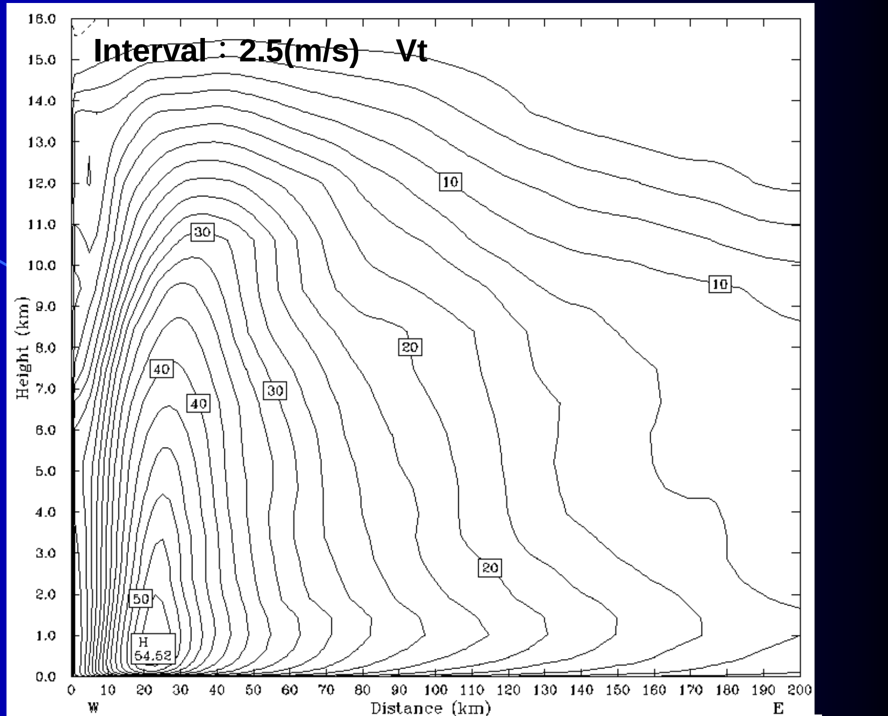
Interval：2.5(m/s)　Vt
Height (km)
Distance (km)
W
E

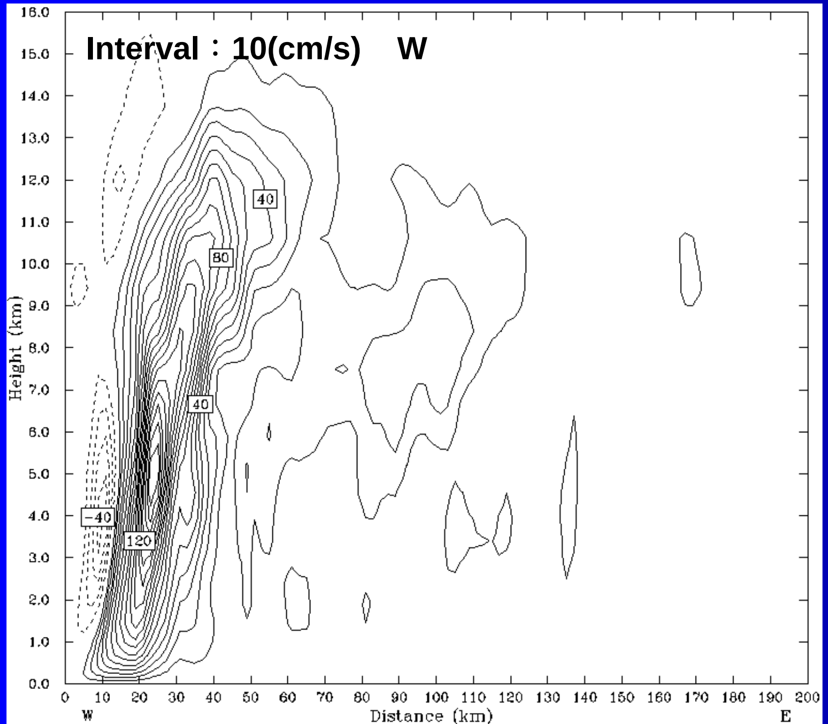
Interval：10(cm/s)　W
Height (km)
Distance (km)
W
E

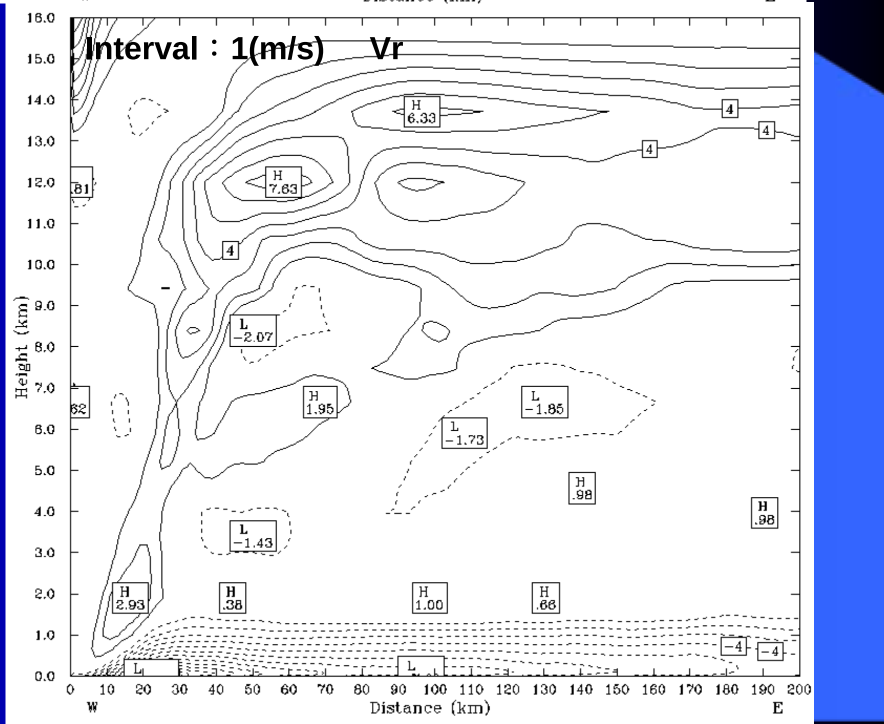
Interval：1(m/s)　Vr
Height (km)
Distance (km)
W
E

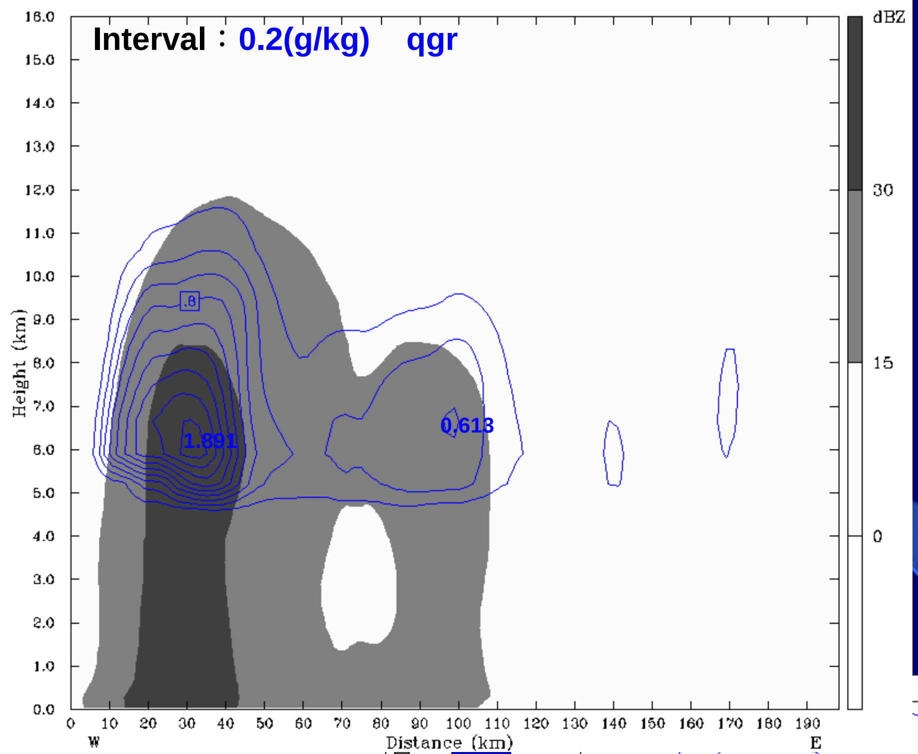

Interval：0.2(g/kg) qgr
1.891
0.613
.8
Height (km)
Distance (km)
W
E
dBZ
30
15
0

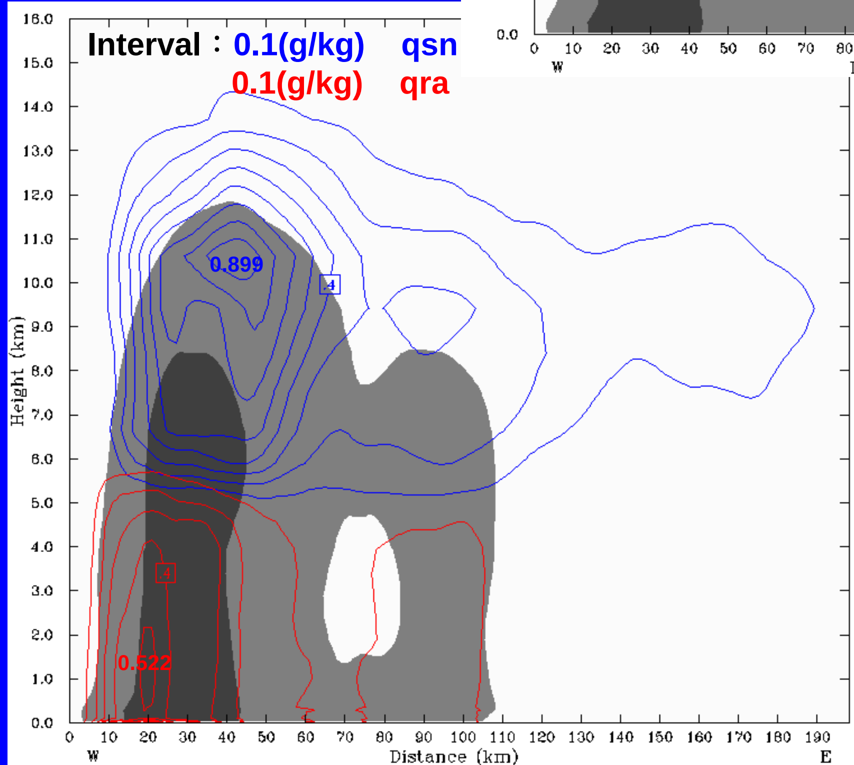

Interval：0.1(g/kg) qsn
0.1(g/kg) qra
0.899
.4
0.522
Height (km)
Distance (km)
W
E
30
15
0

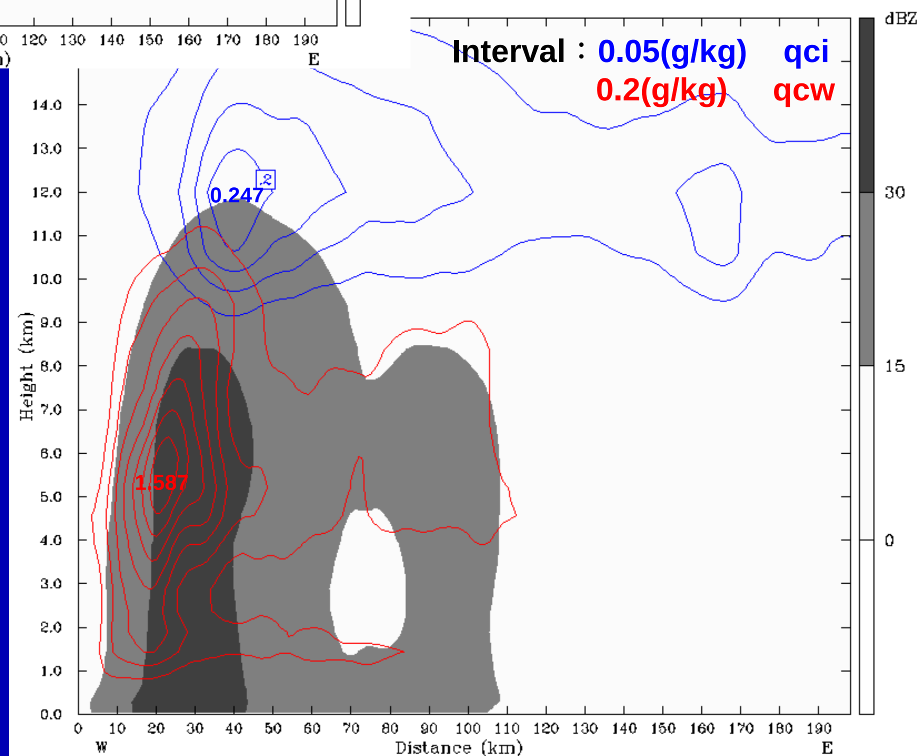

Interval：0.05(g/kg) qci
0.2(g/kg) qcw
0.247
.2
1.587
Height (km)
Distance (km)
W
E
dBZ
30
15
0

Landfall Stage
(2 Hours After Landfall)

Semicircle-avg. structure (r=180 km)
Nari is at landfall

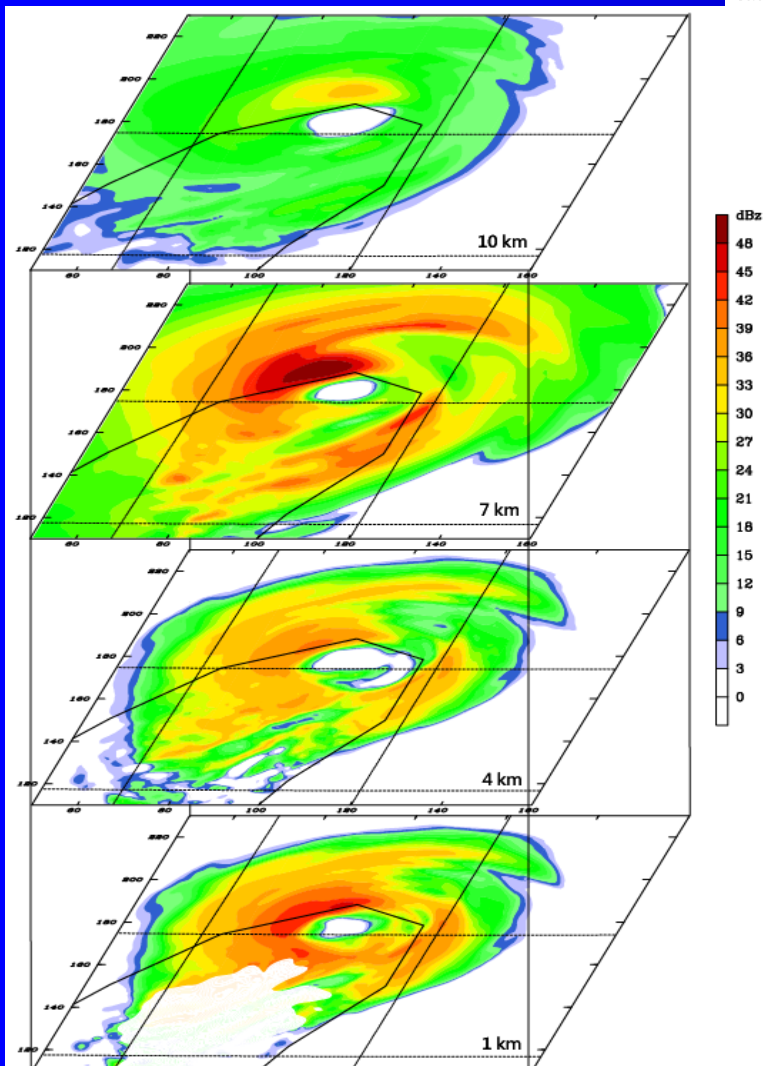

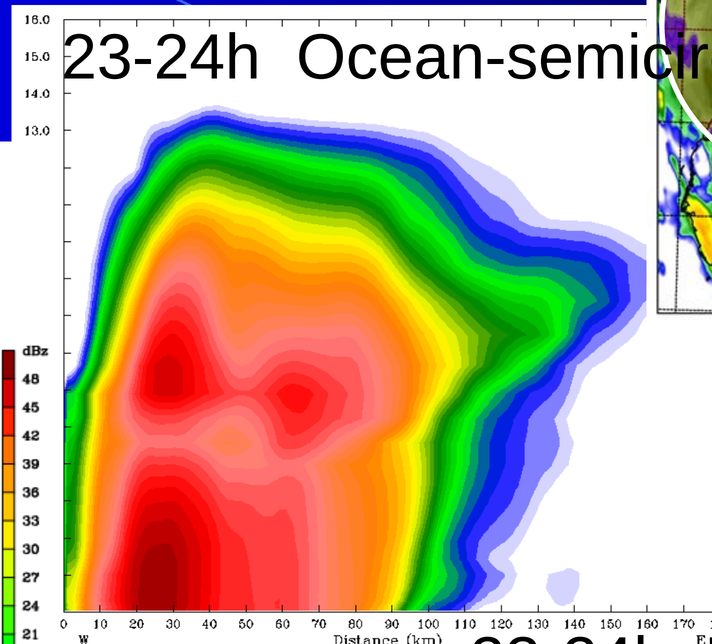

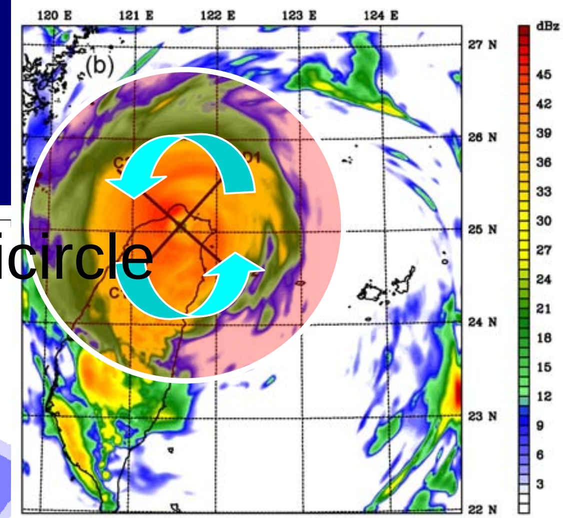

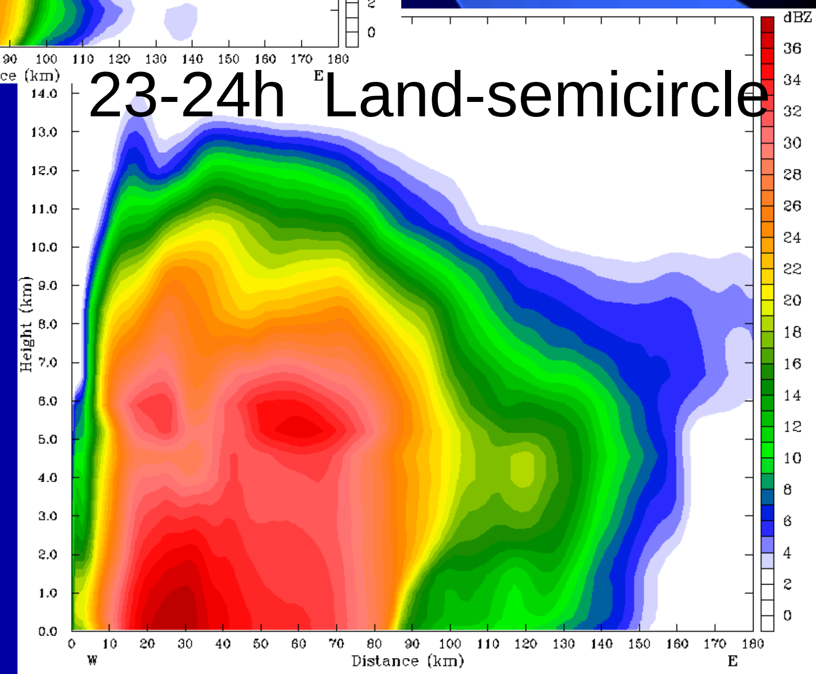

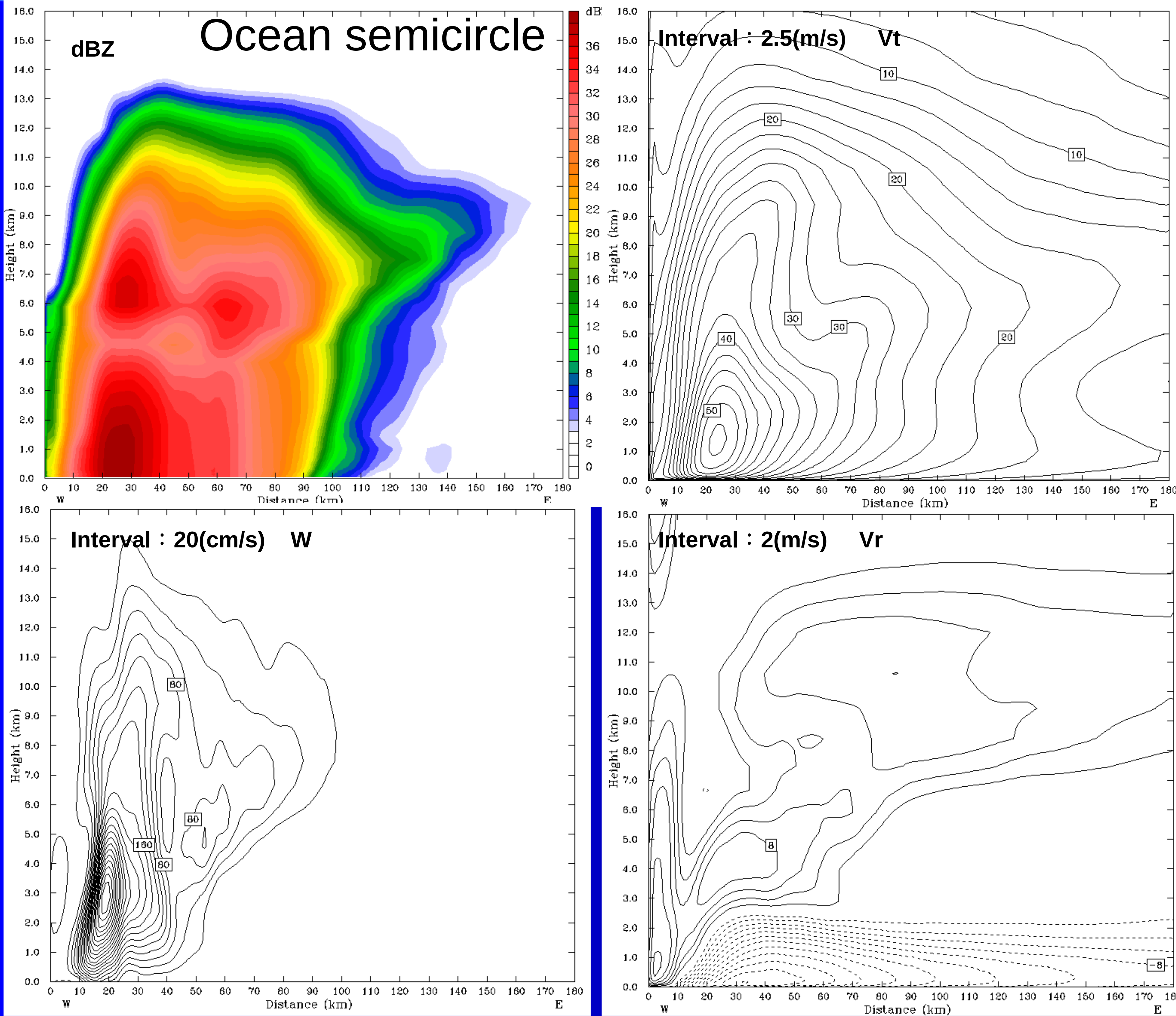
Ocean semicircle
dBZ
Interval：2.5(m/s)　Vt
Interval：20(cm/s)　W
Interval：2(m/s)　Vr
Height (km)
Distance (km)
W
E

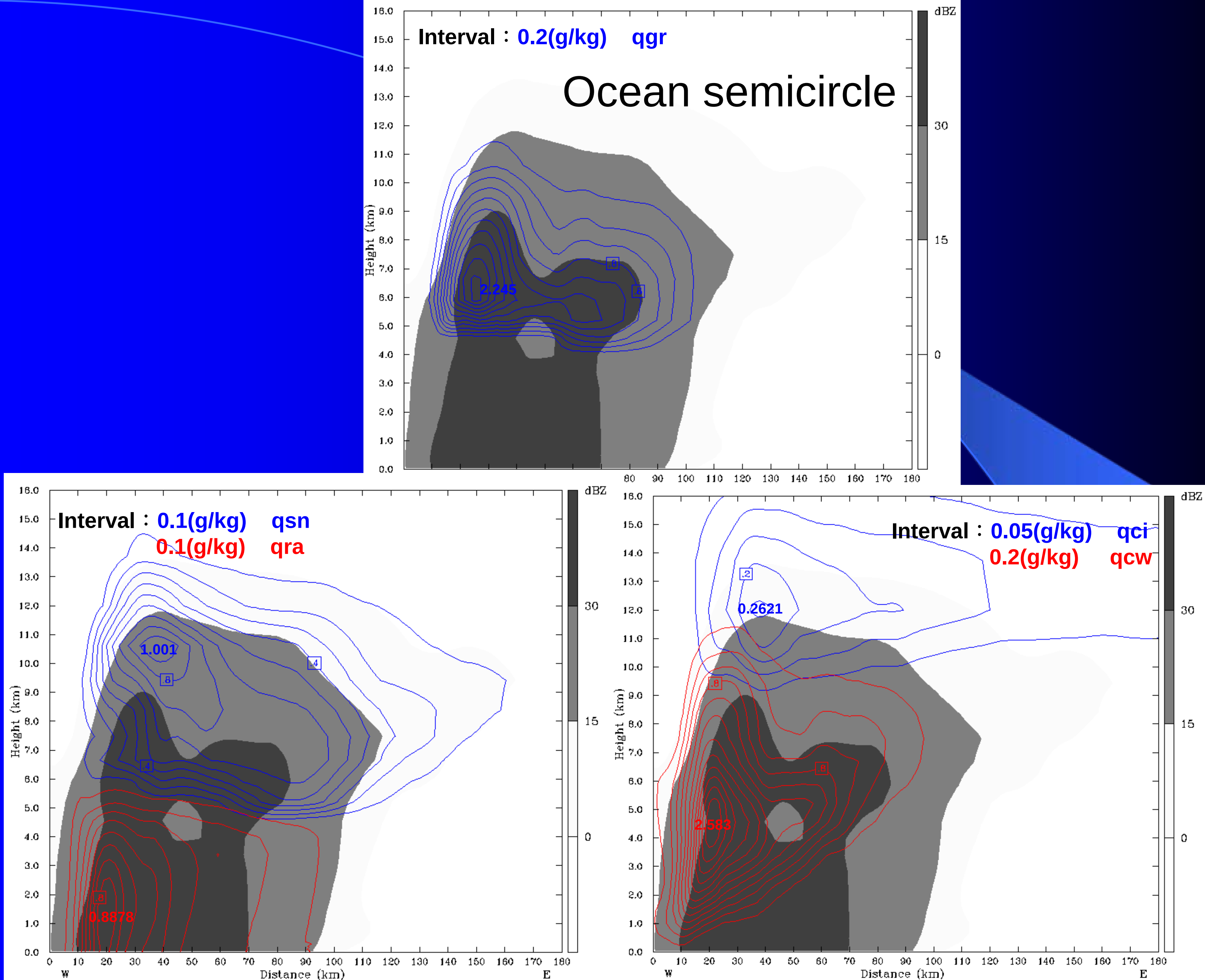

Interval：0.2(g/kg) qgr
Ocean semicircle
2.245
Interval：0.1(g/kg) qsn
0.1(g/kg) qra
1.001
0.8878
Interval：0.05(g/kg) qci
0.2(g/kg) qcw
0.2621
2.583
Height (km)
Distance (km)
dBZ
W
E

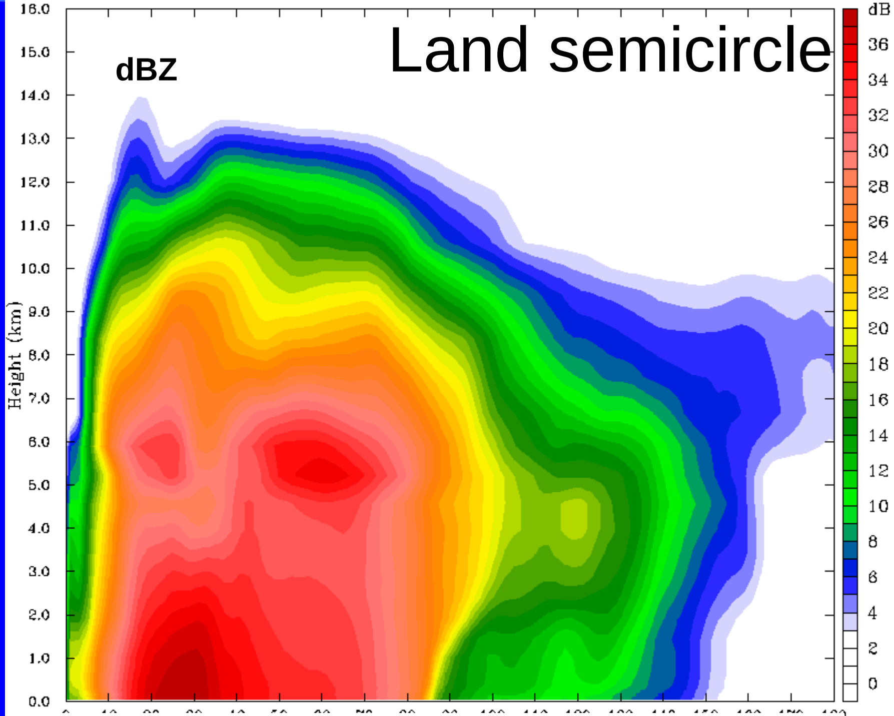
Land semicircle
dBZ
Height (km)
dB

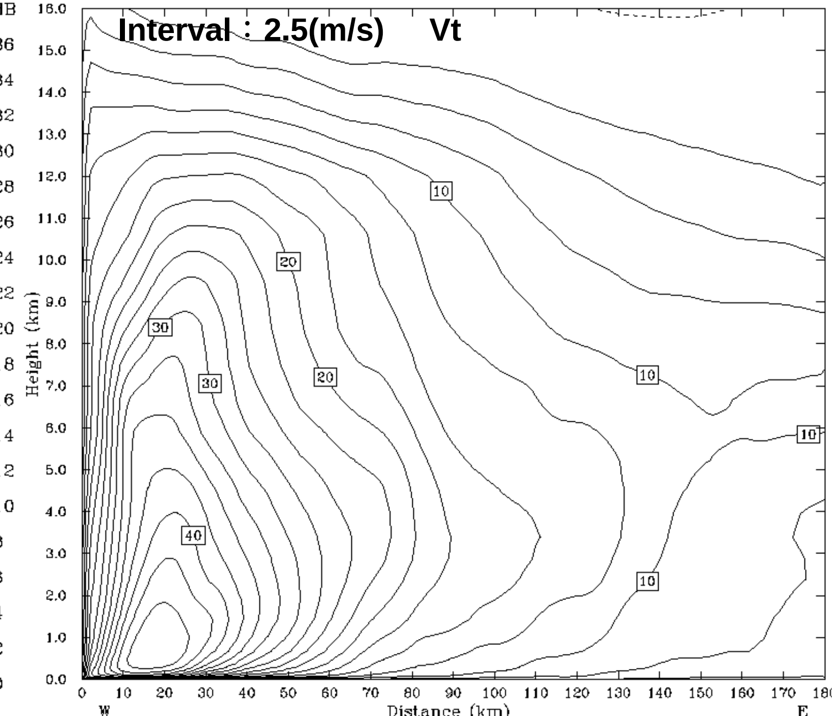
Interval：2.5(m/s)　Vt
Height (km)
Distance (km)
W
E
10
20
30
40

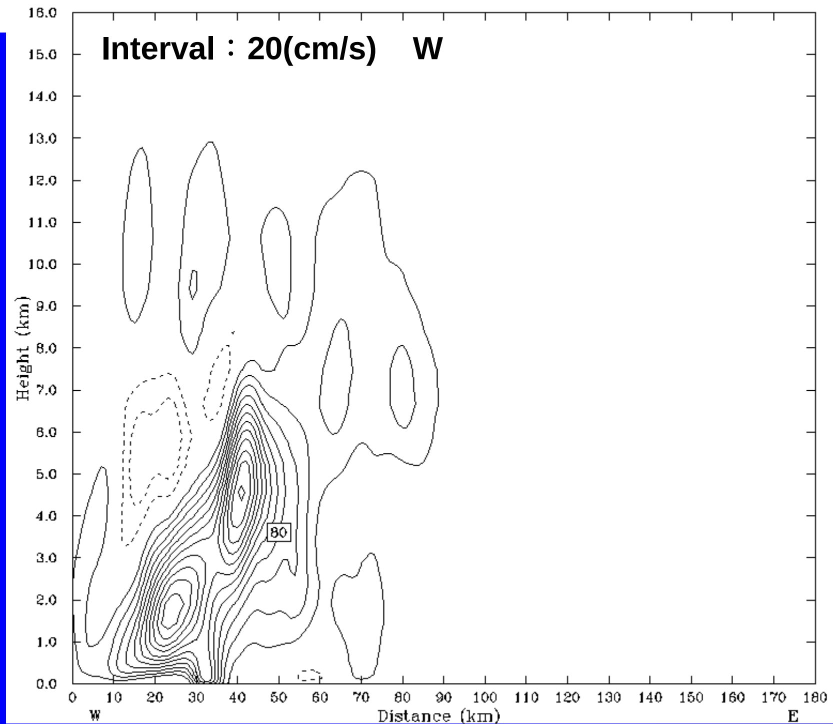
Interval：20(cm/s)　W
Height (km)
Distance (km)
W
E
80

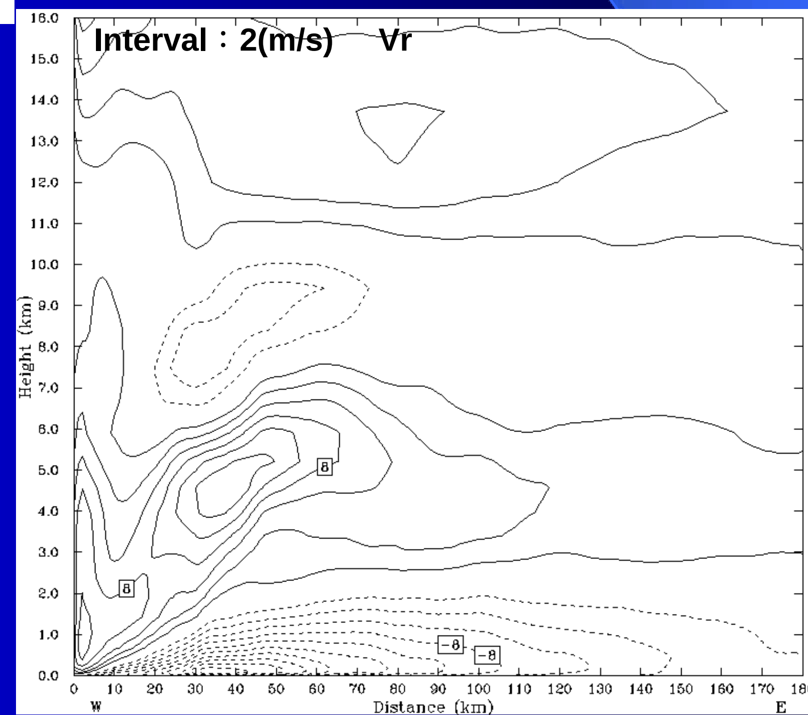
Interval：2(m/s)　Vr
Height (km)
Distance (km)
W
E
8
-8

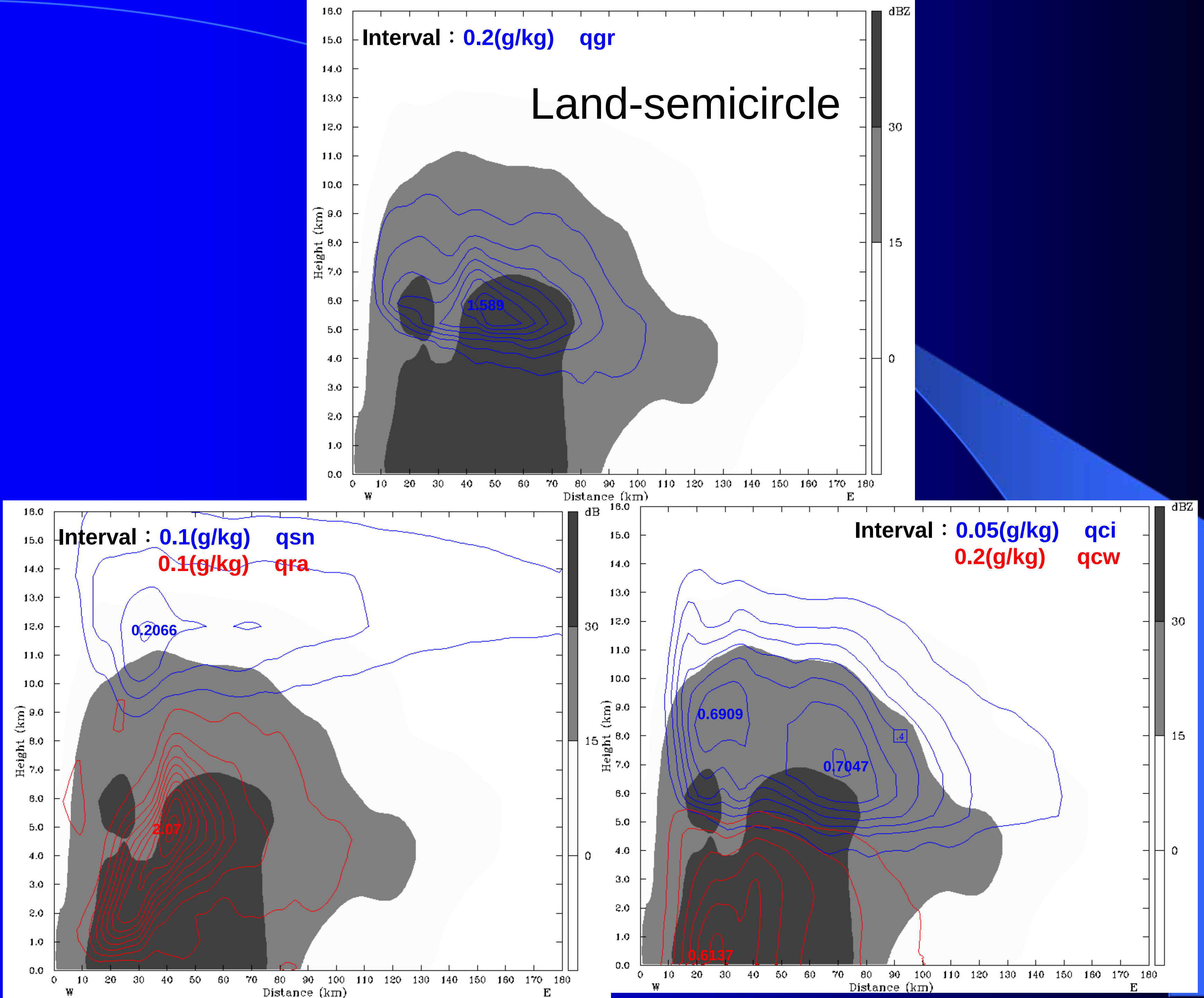

Interval：0.2(g/kg) qgr
Land-semicircle
1.589
Interval：0.1(g/kg) qsn
0.1(g/kg) qra
0.2066
2.07
Interval：0.05(g/kg) qci
0.2(g/kg) qcw
0.6909
0.7047
0.6137
Height (km)
Distance (km)
W
E
dBZ
30
15
0

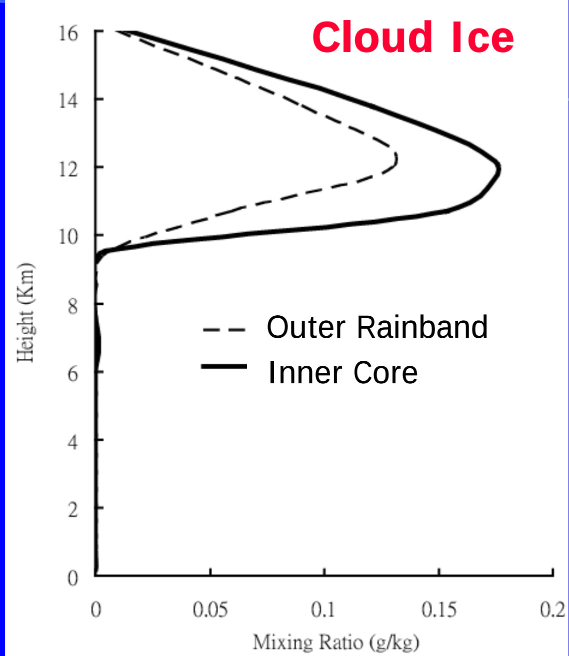

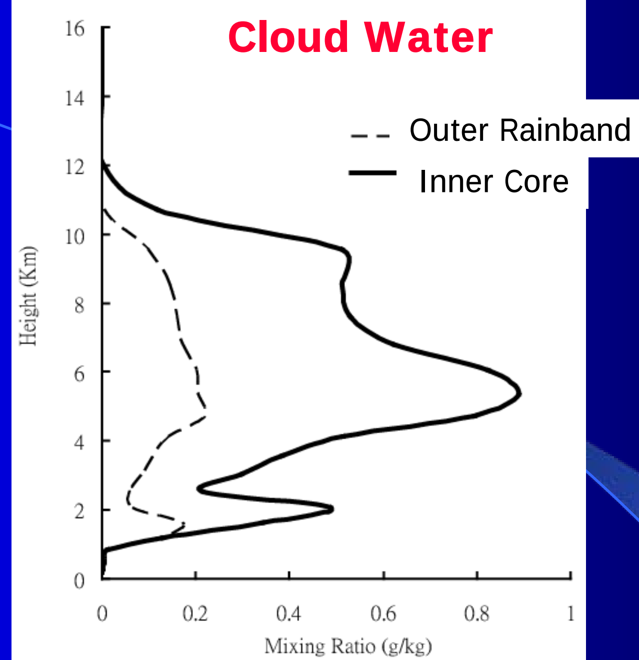

9 h Before Landfall

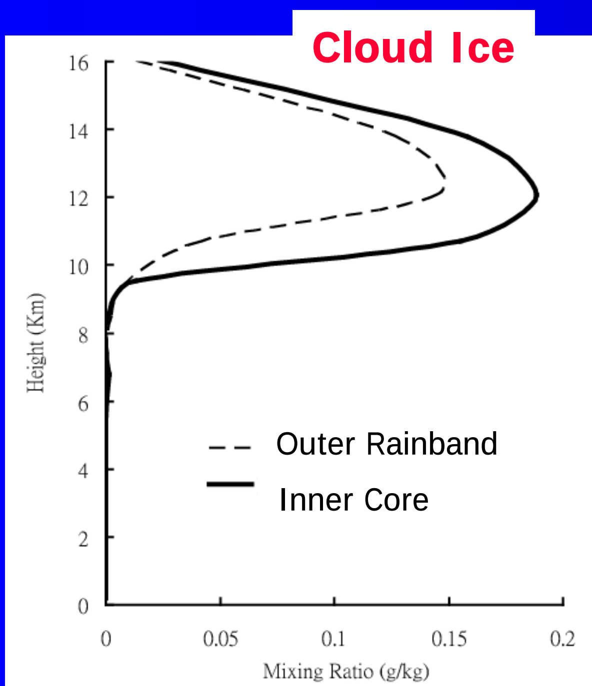

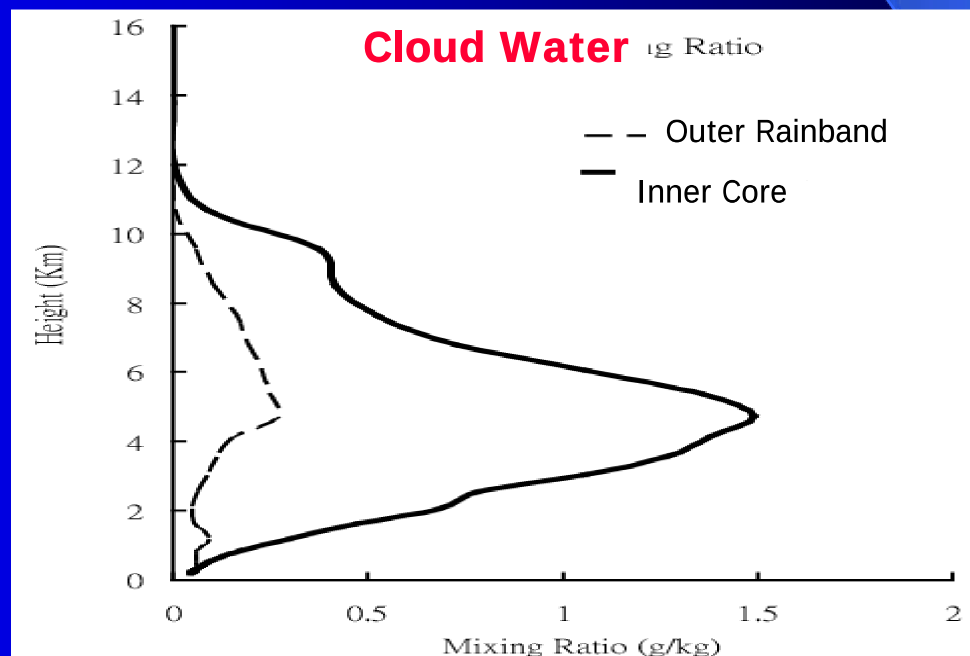

2 h After Landfall

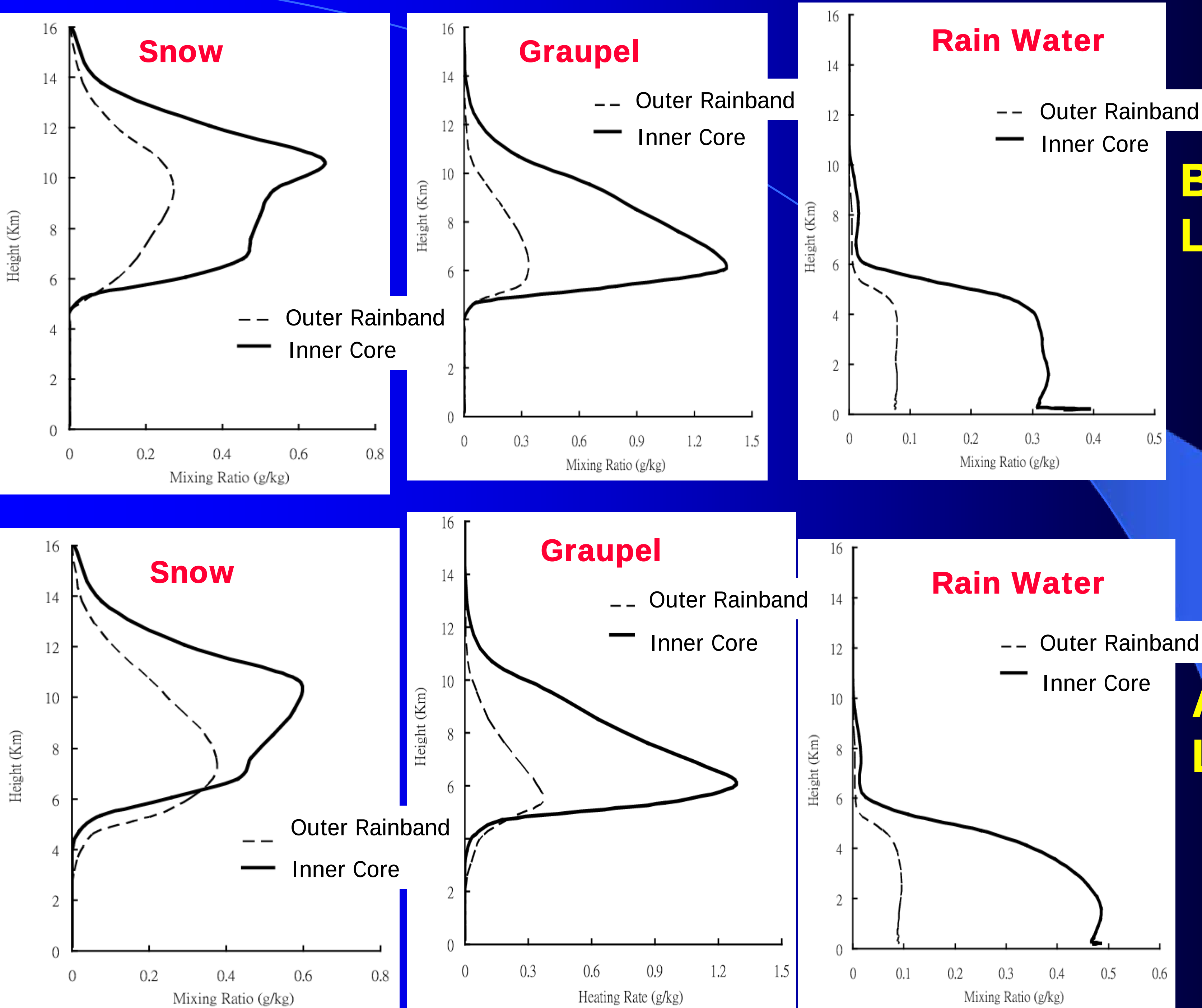

Before Landfall

After Landfall

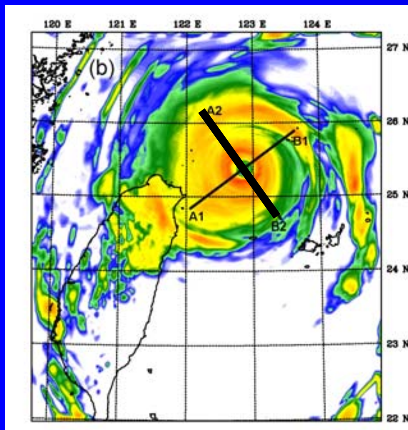

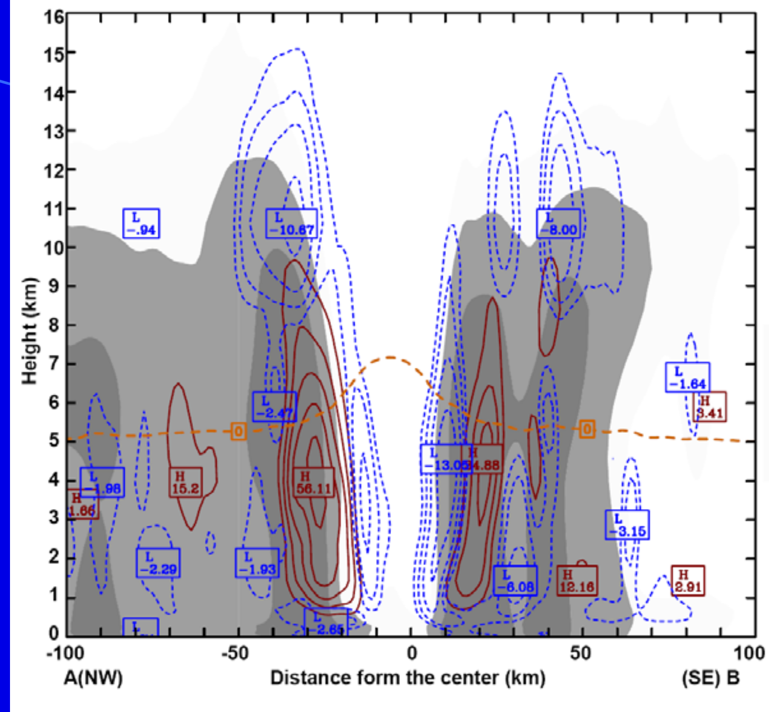

Before Landfall

Condensation Heating (solid line)
Evaporation Cooling (dashed line)

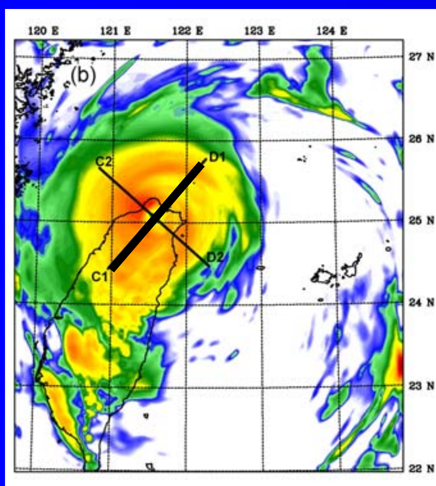

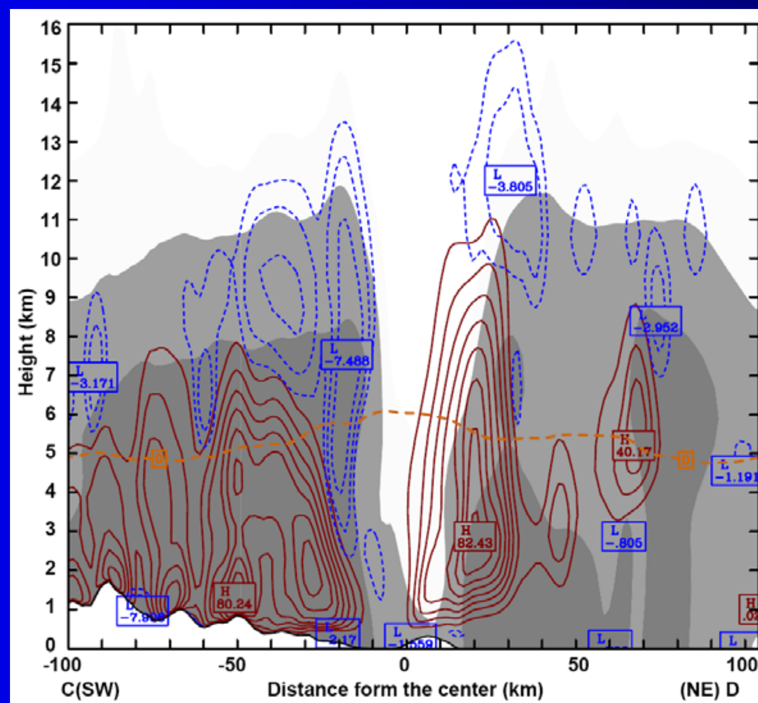

After Landfall

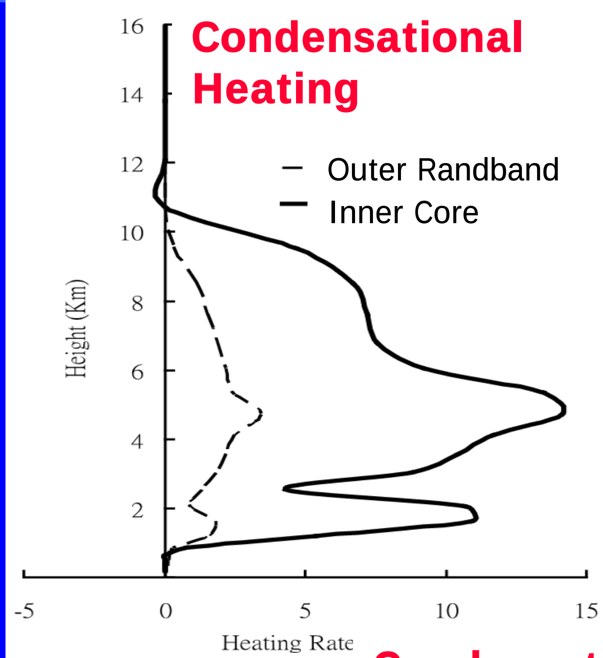

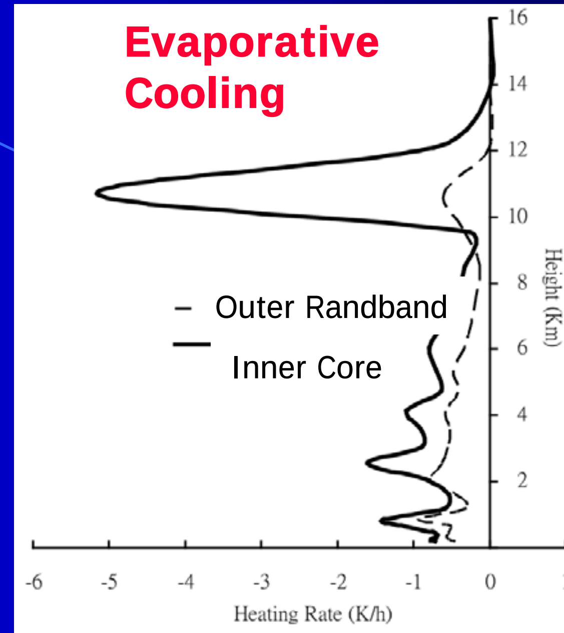

Before Landfall

Condensation Heating

Evaporative Cooling

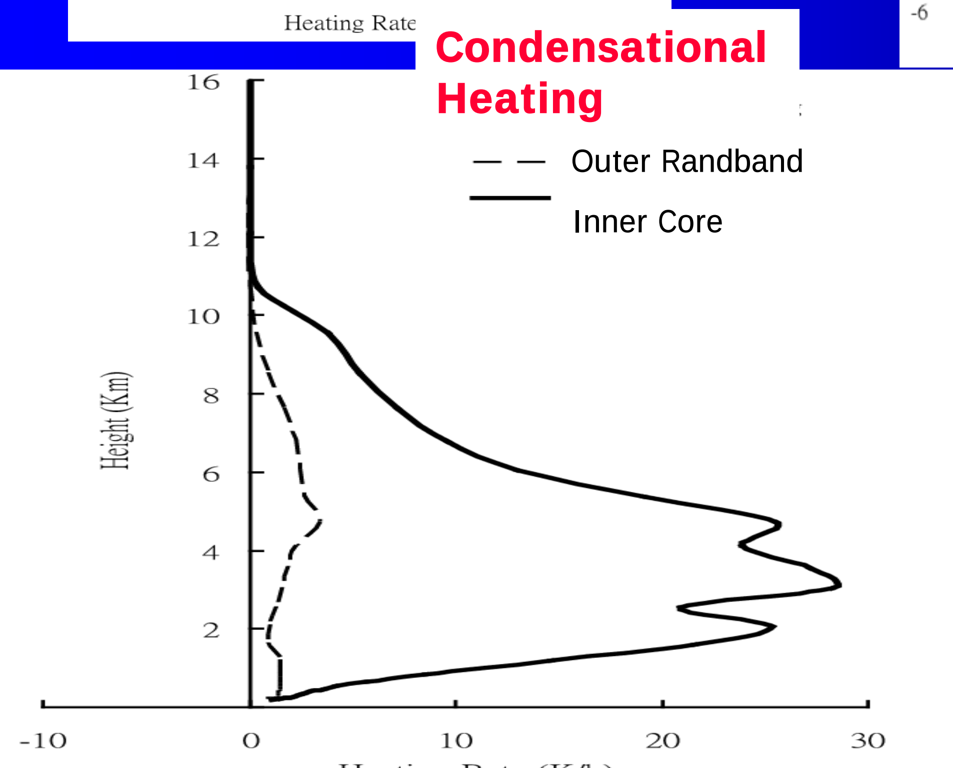

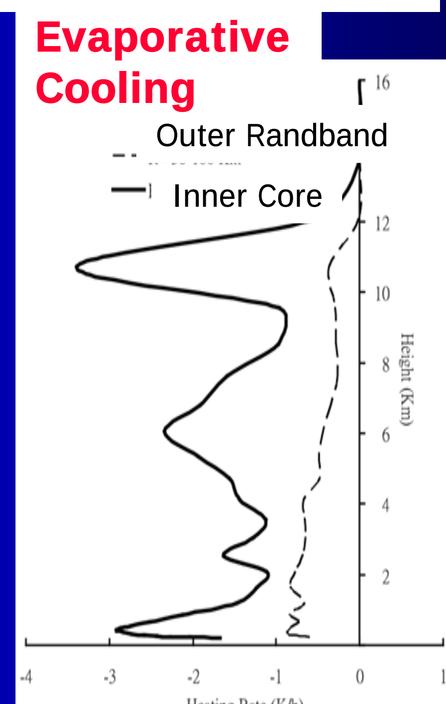

After Landfall

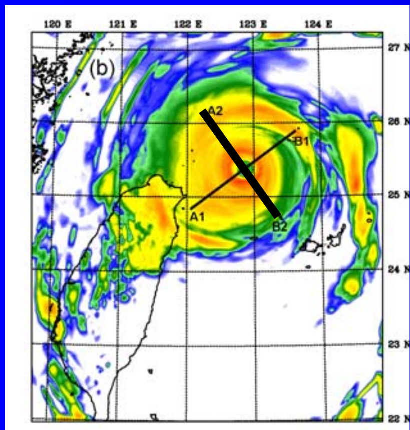

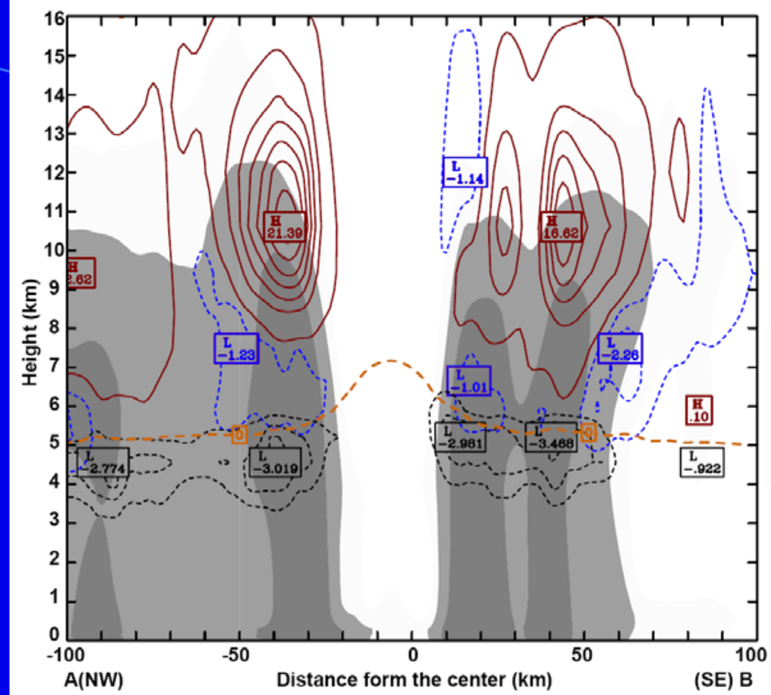

Before Landfall

Deposition Heating (solid black)

Sublimative Cooling (dashed blue)

Melting Cooling (dashed black)

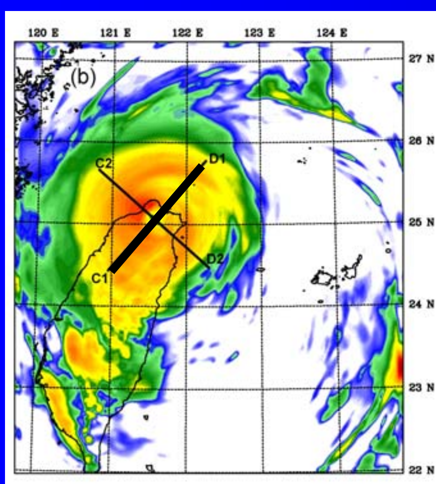

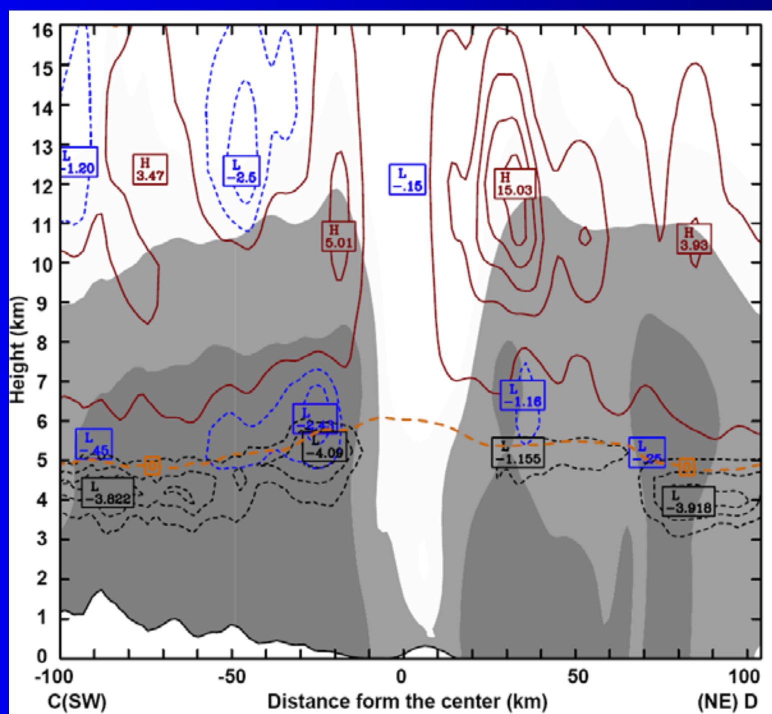

After Landfall

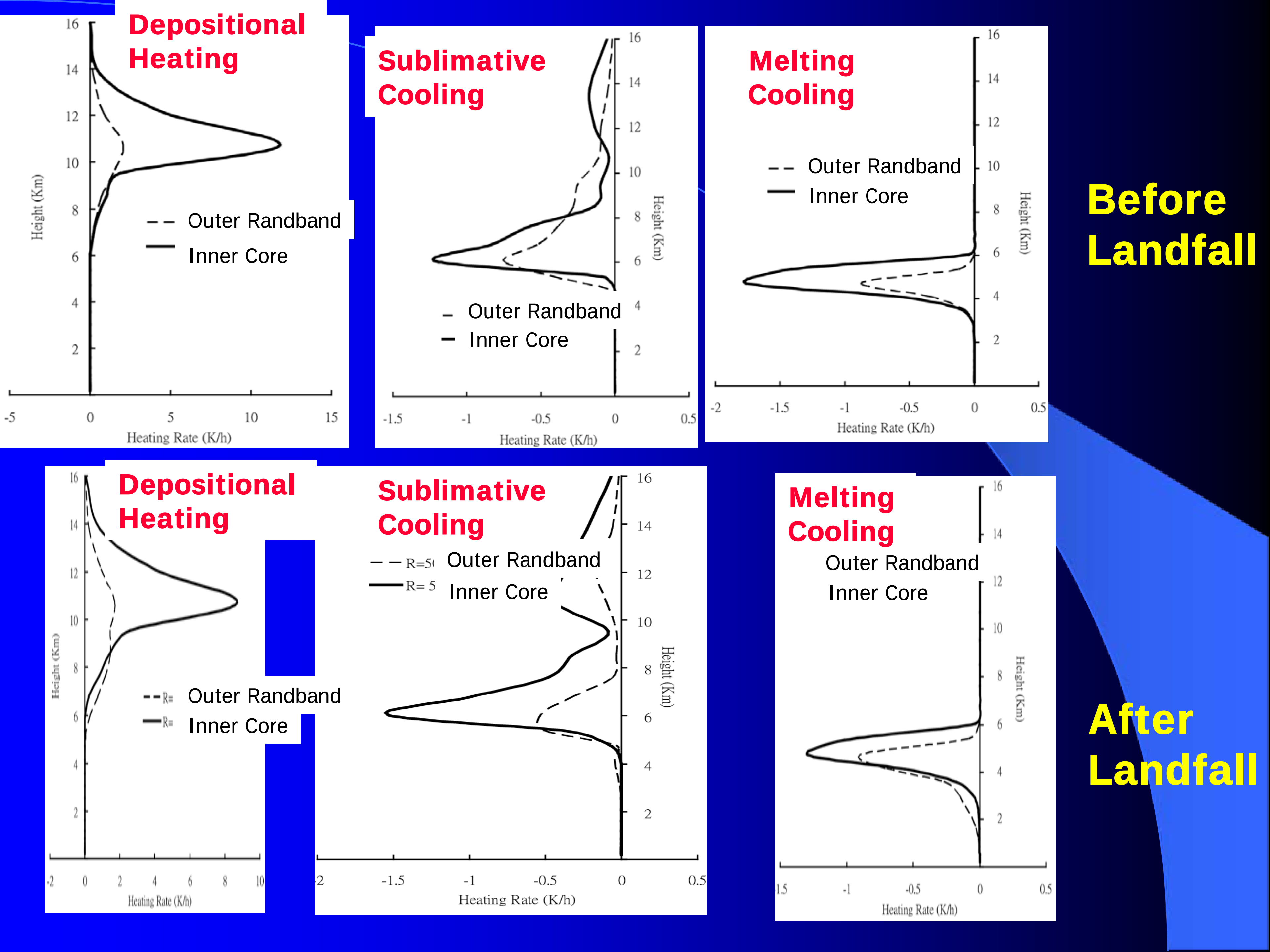

Depositional Heating
Outer Randband
Inner Core
Height (Km)
Heating Rate (K/h)
Sublimative Cooling
Outer Randband
Inner Core
Height (Km)
Heating Rate (K/h)
Melting Cooling
Outer Randband
Inner Core
Height (Km)
Heating Rate (K/h)
Before Landfall
Depositional Heating
Outer Randband
Inner Core
Height (Km)
Heating Rate (K/h)
Sublimative Cooling
Outer Randband
Inner Core
Height (Km)
Heating Rate (K/h)
Melting Cooling
Outer Randband
Inner Core
Height (Km)
Heating Rate (K/h)
After Landfall

Before Landfall

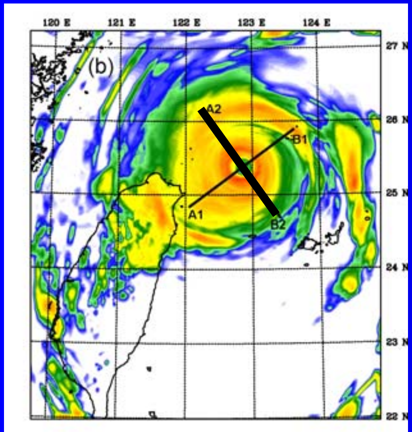

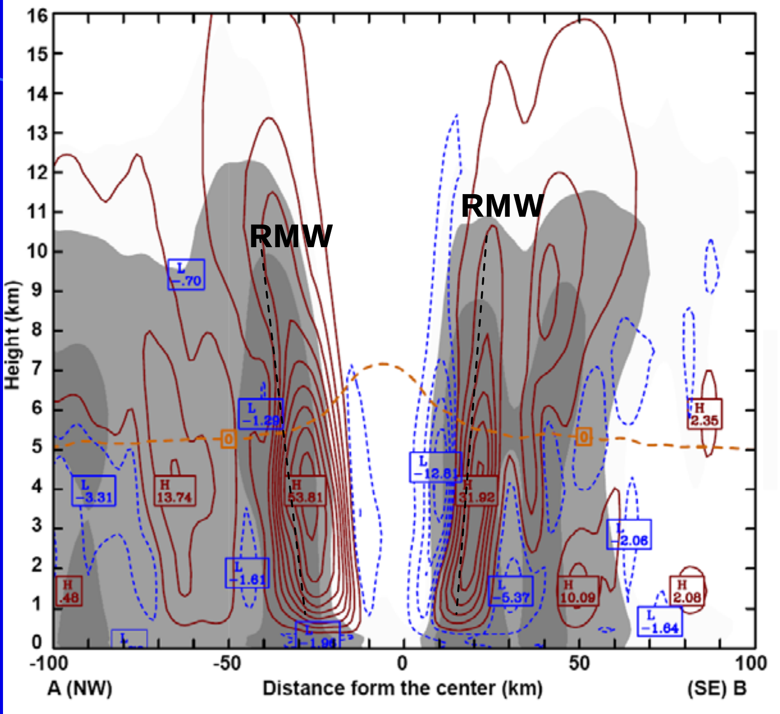

Total Latent Heating (solid black)

Total Latent Cooling (dashed blue)

After Landfall

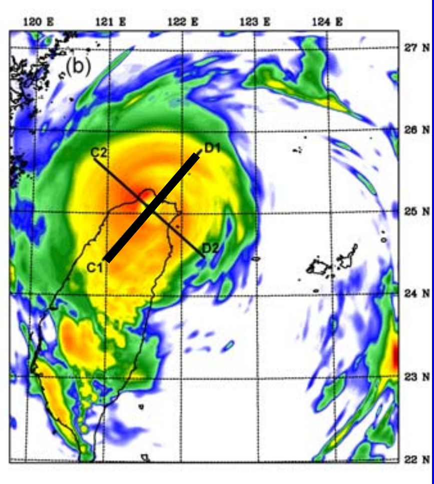

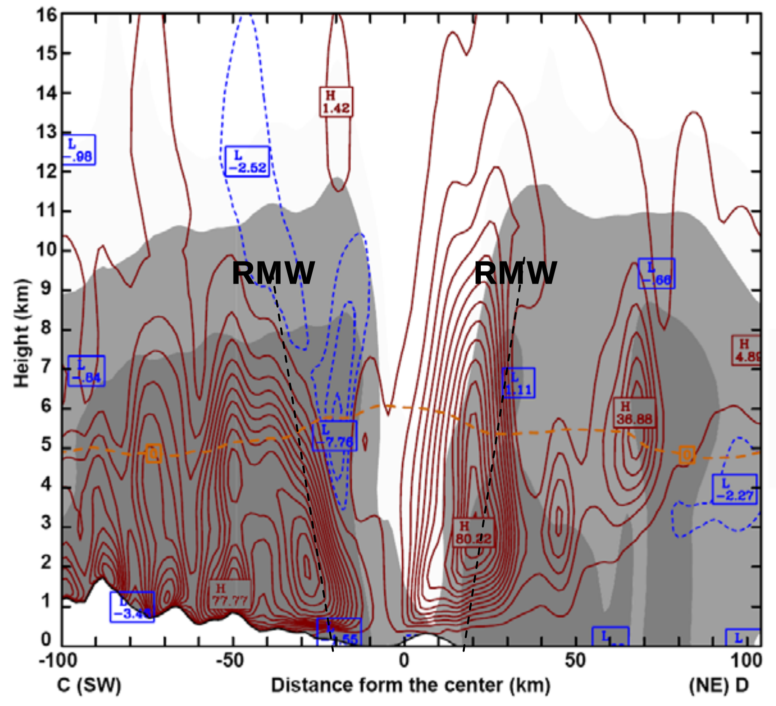

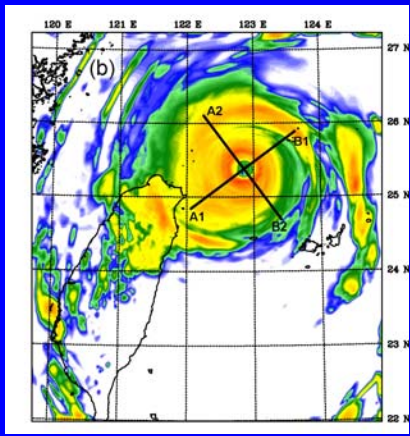

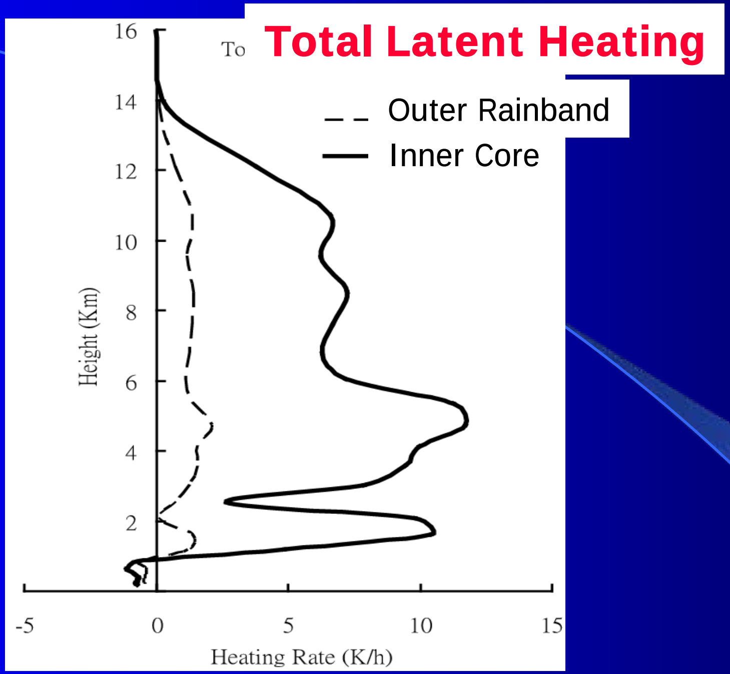

Before Landfall

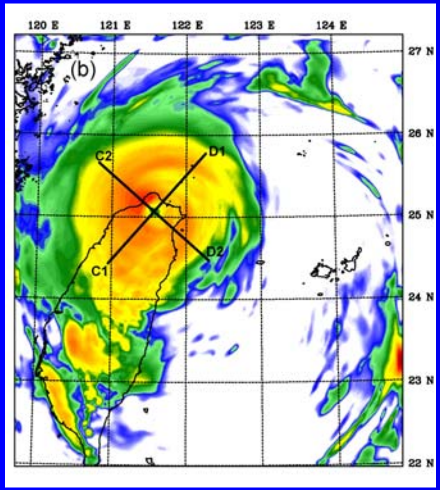

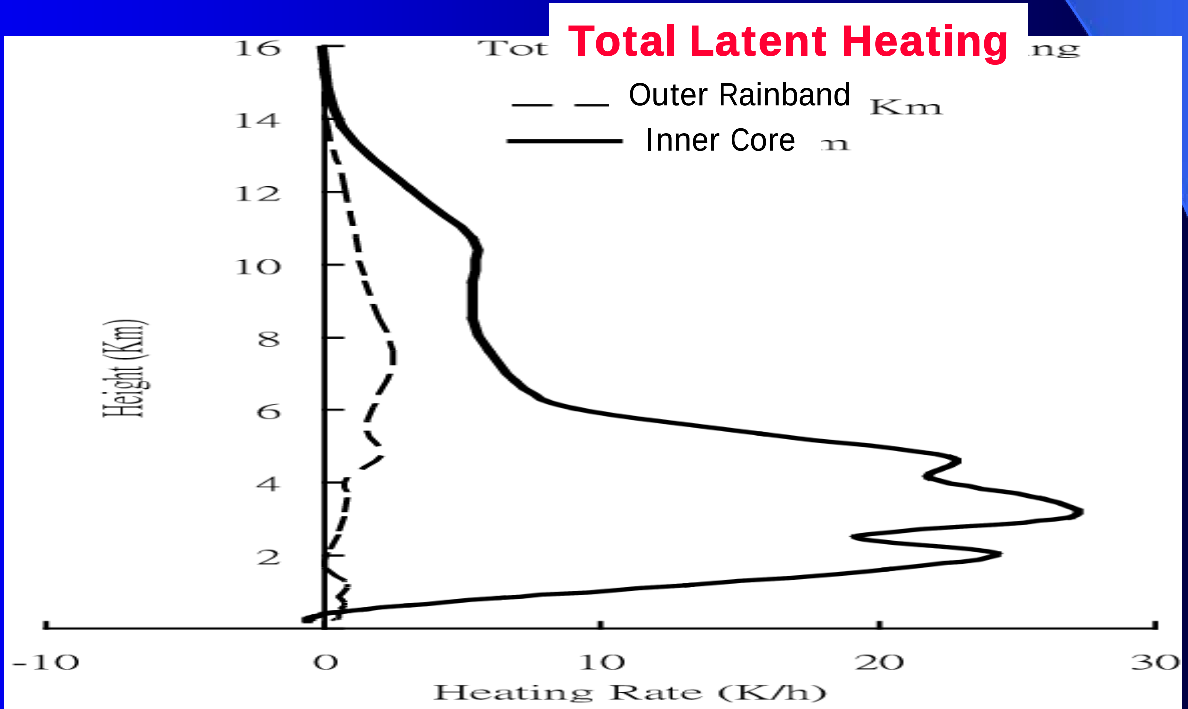

After Landfall

Midlatitude MCS/Cv

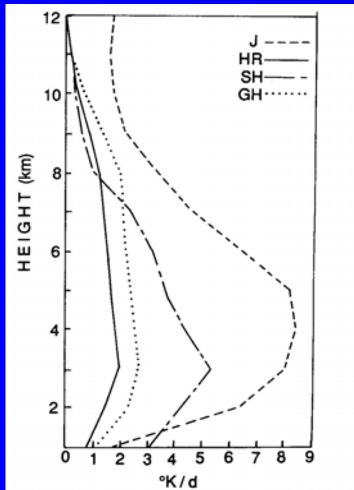

Houze (1989; QJRMS)

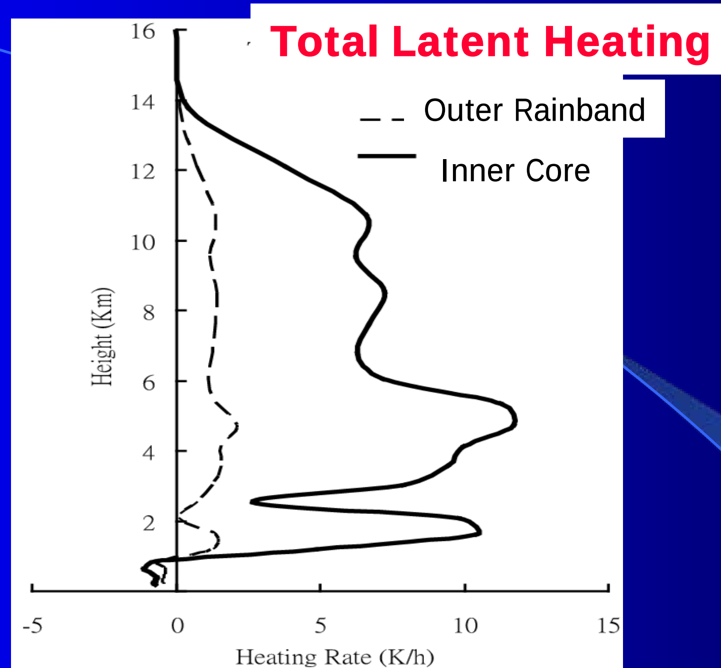

Before Landfall

Total Latent Heating
& Cooling

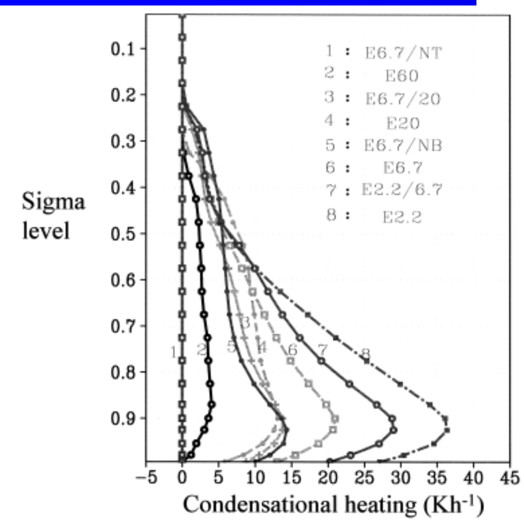

Fig. 12. Same as Fig. 11 but for condensational heating (K h^{-1}).

Wu et al. (2002; WAF)

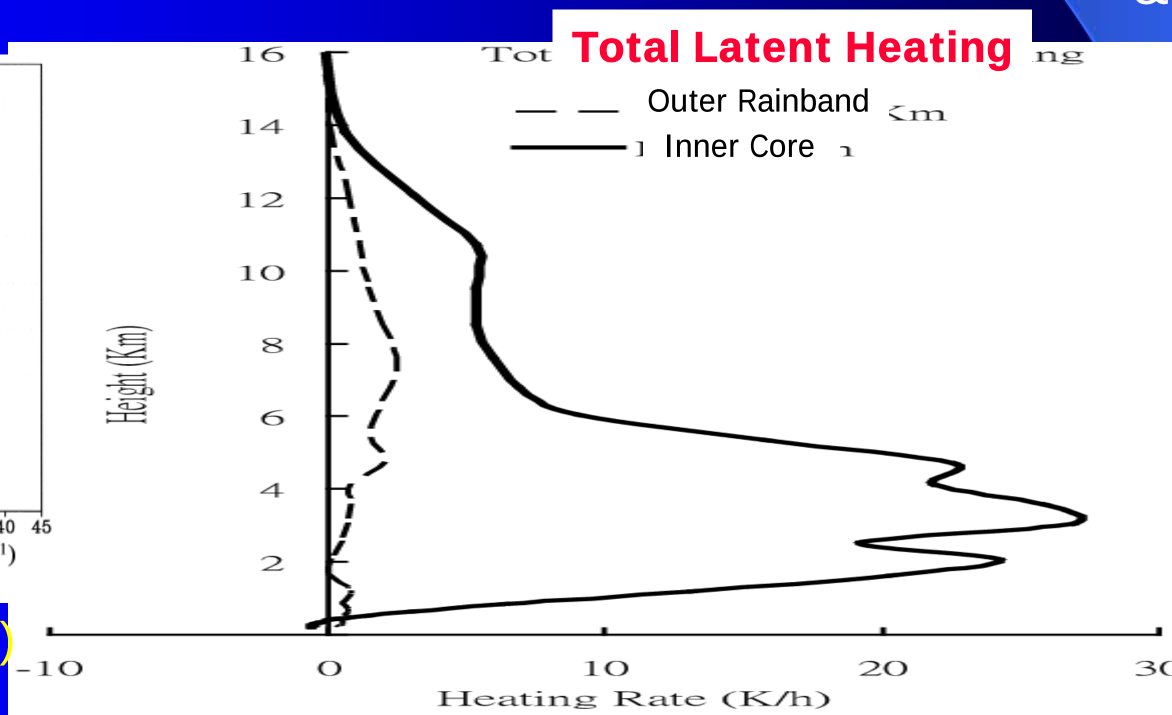

After Landfall

Storm Contraction during Landfall

Shrinkage of Typhoon Eye

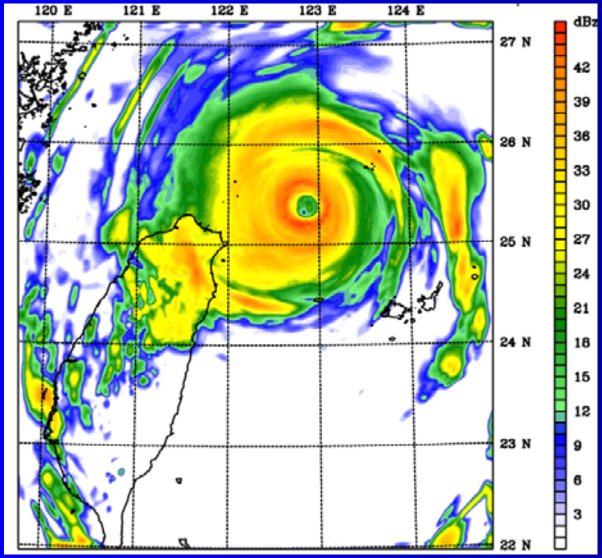

MM5 Radar CV @ 9/16 0130Z
(1-h time averaged)

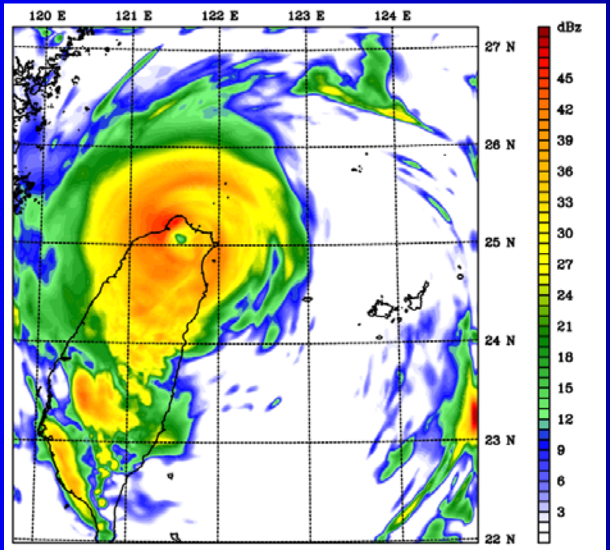

MM5 Radar CV @ 9/16 1200Z
(1-h time averaged)

Hovmoller Diagram of Azimuthal-Avg. Wind

Near-Surface
Tangential Wind (V')

Landfall

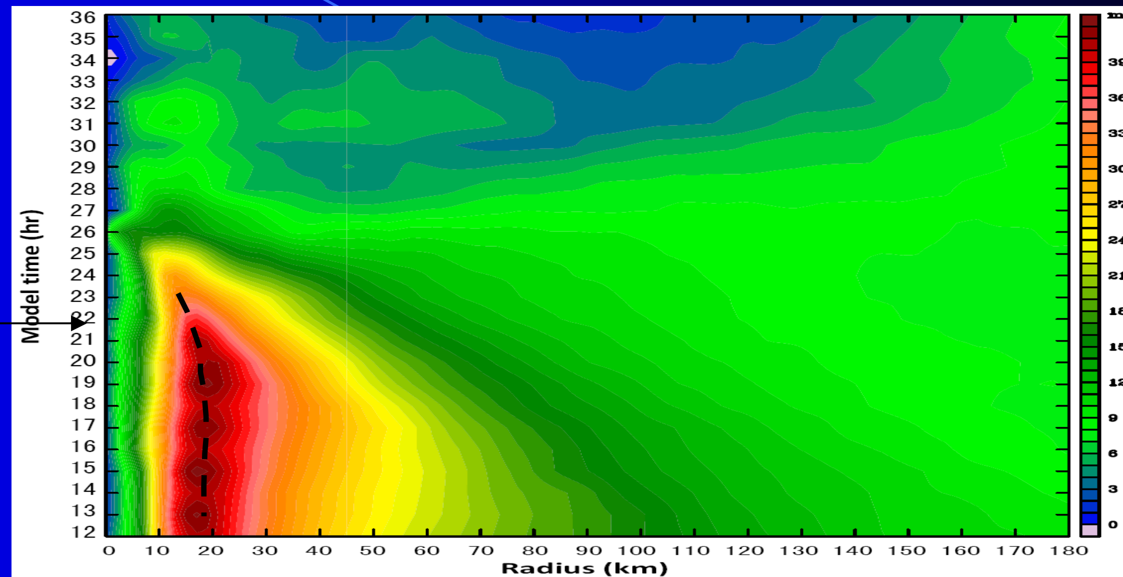

Landfall

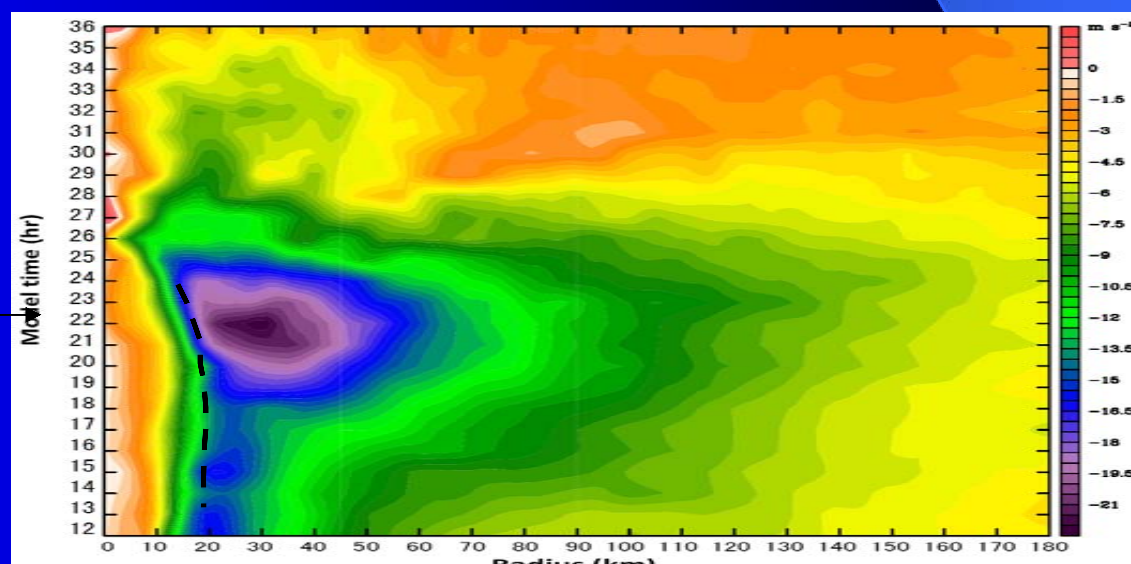

Near-Surface
Radial Wind (U')

Time Series of Vertical Profiles of Vertical Velocity within the Eye

Averaged over a Square of 12 km x 12 km centered on the Eye

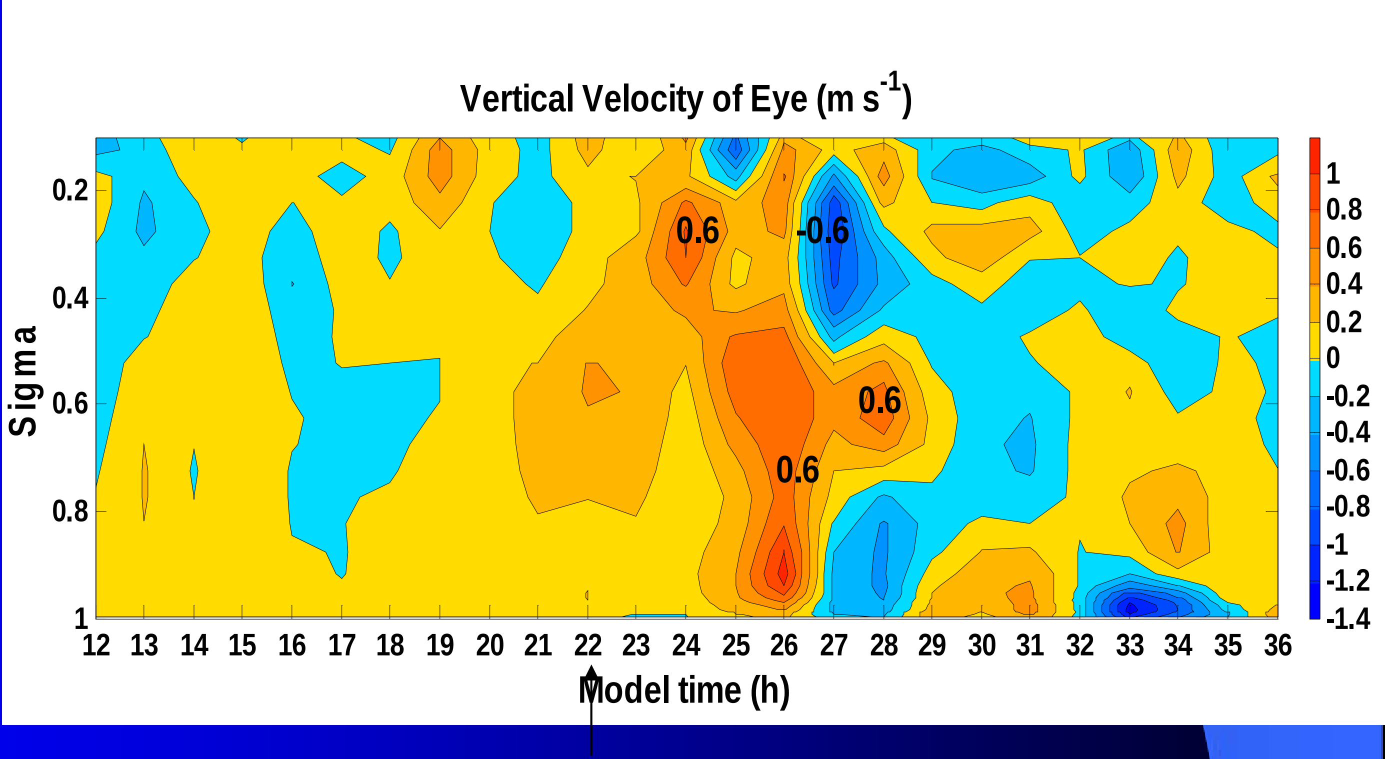

Landfall

Hovmoller Diagram of Horizontal Wind

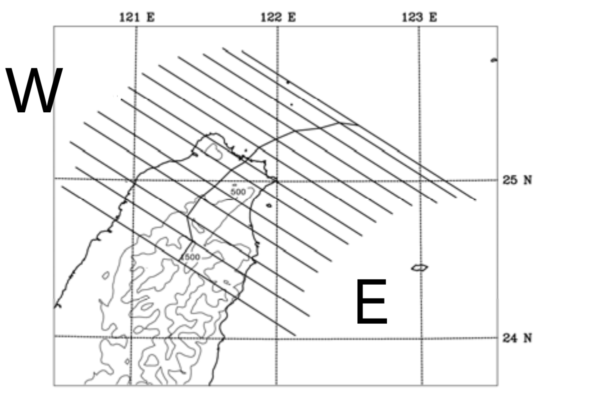

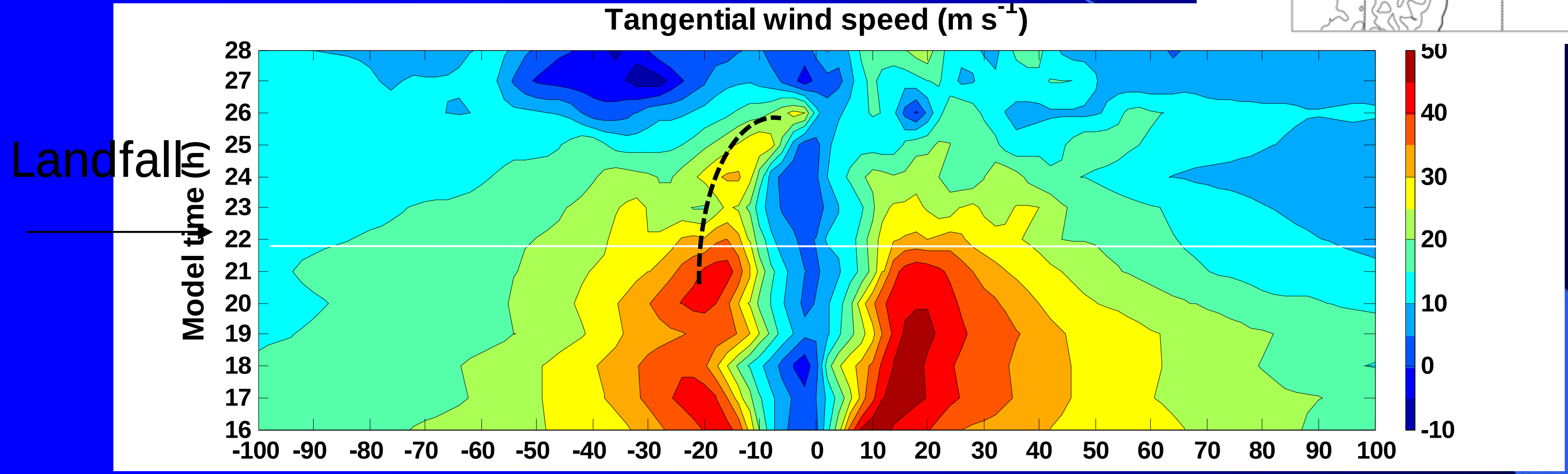

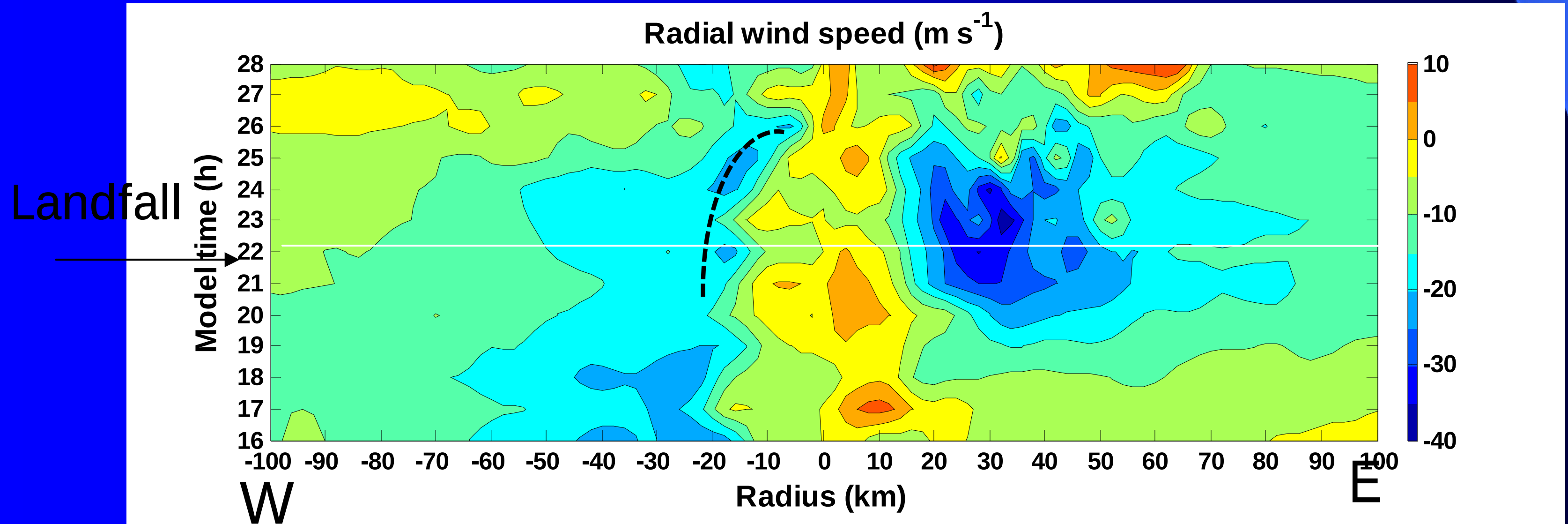

Hovmoller Diagram of Azimuthal-Avg. Wind (No Terrain Experiment)

Near-Surface Tangential Wind (V')

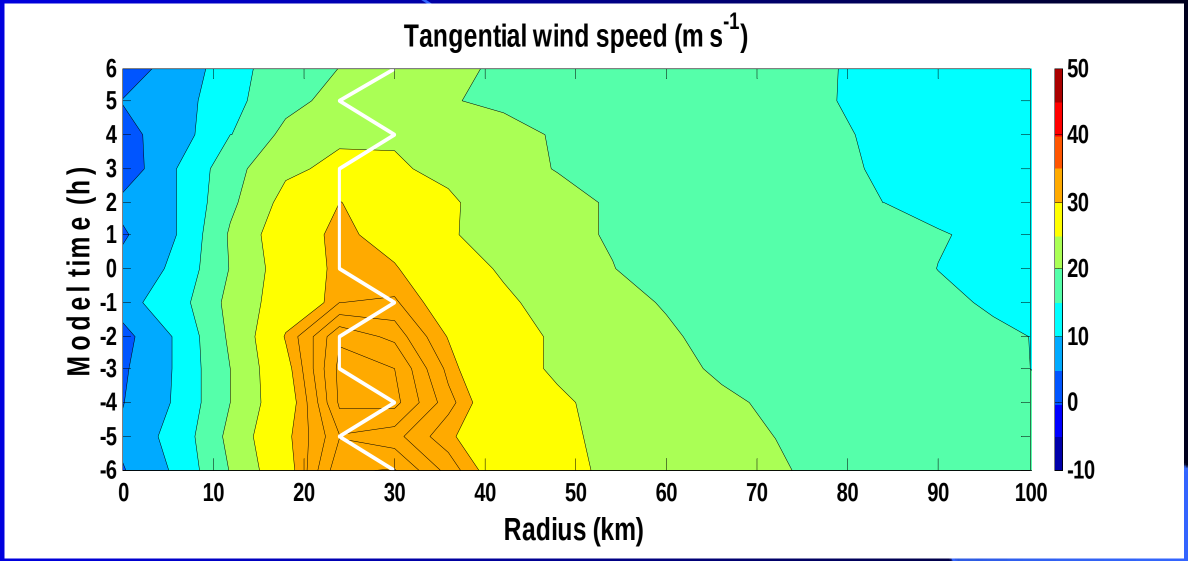

Near-Surface Radial Wind (U')

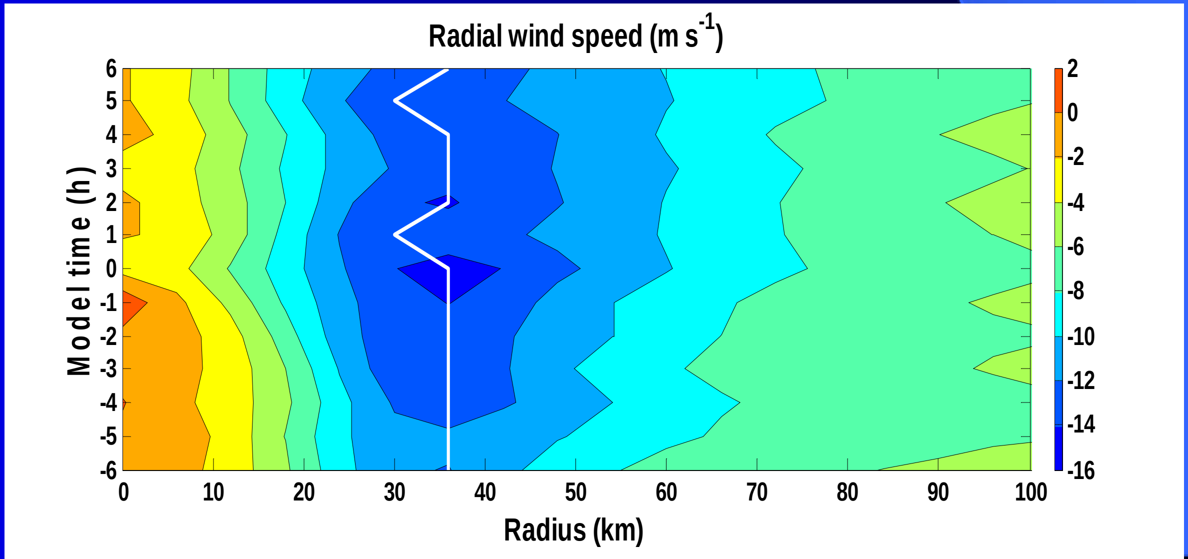

Hovmoller Diagram of Horizontal Wind (No Terrain Experiment)

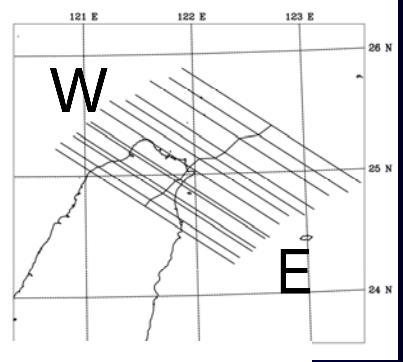

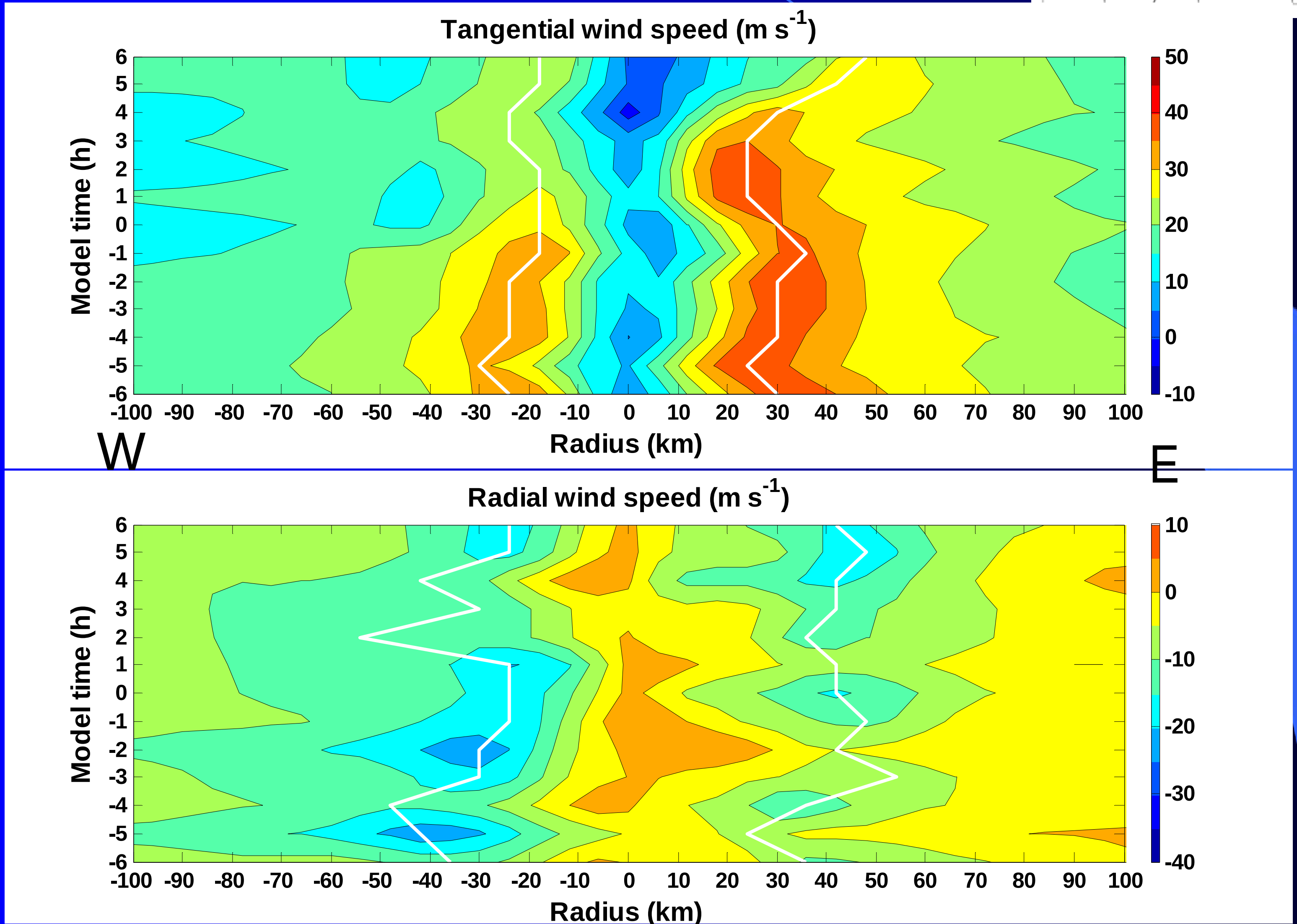

Evolution of Radial Flows

Azimuthal-Avg. Radial Wind (r=180 km)

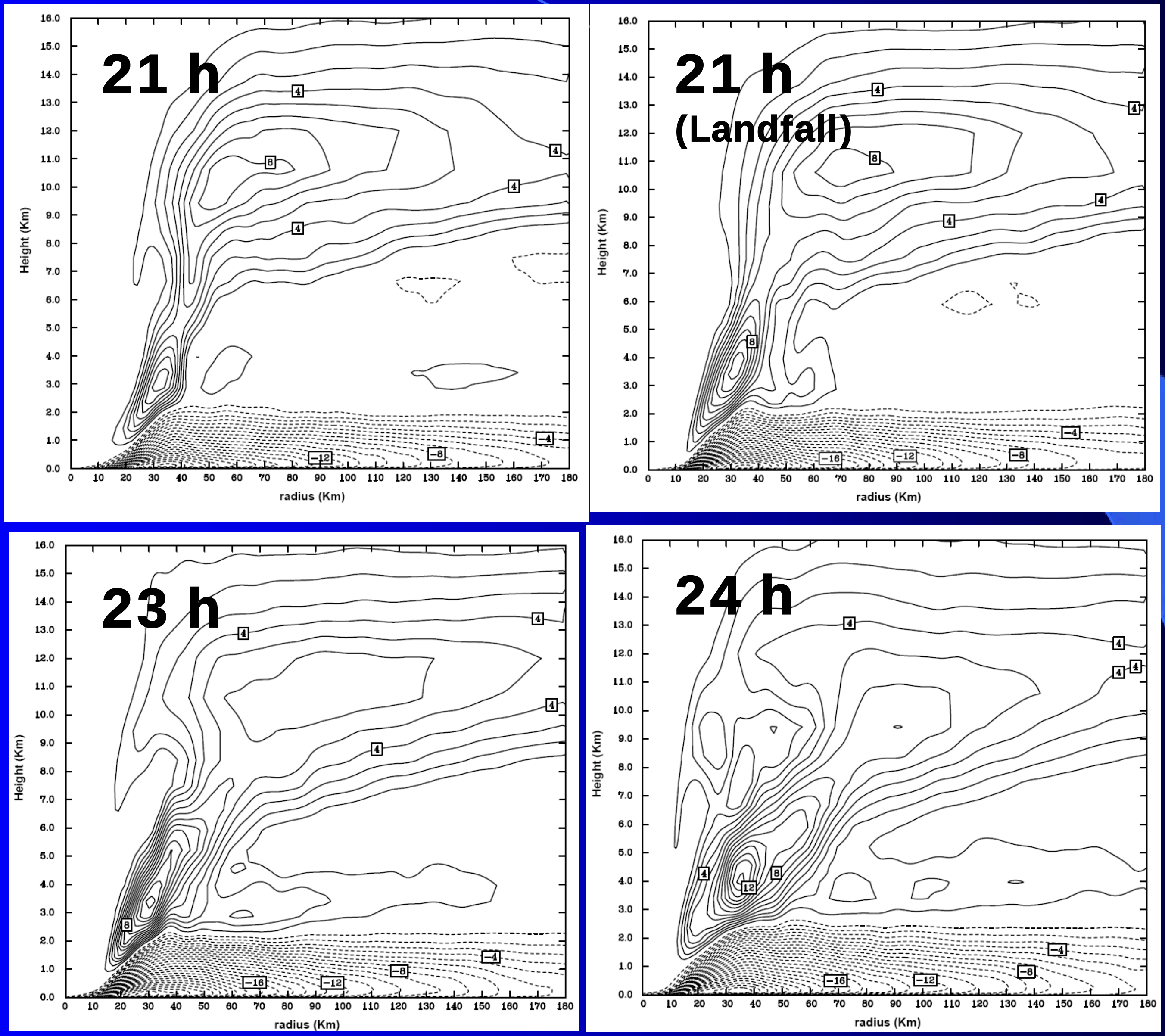

Azimuthal-Avg. Radial Wind
(1 h after landfall)

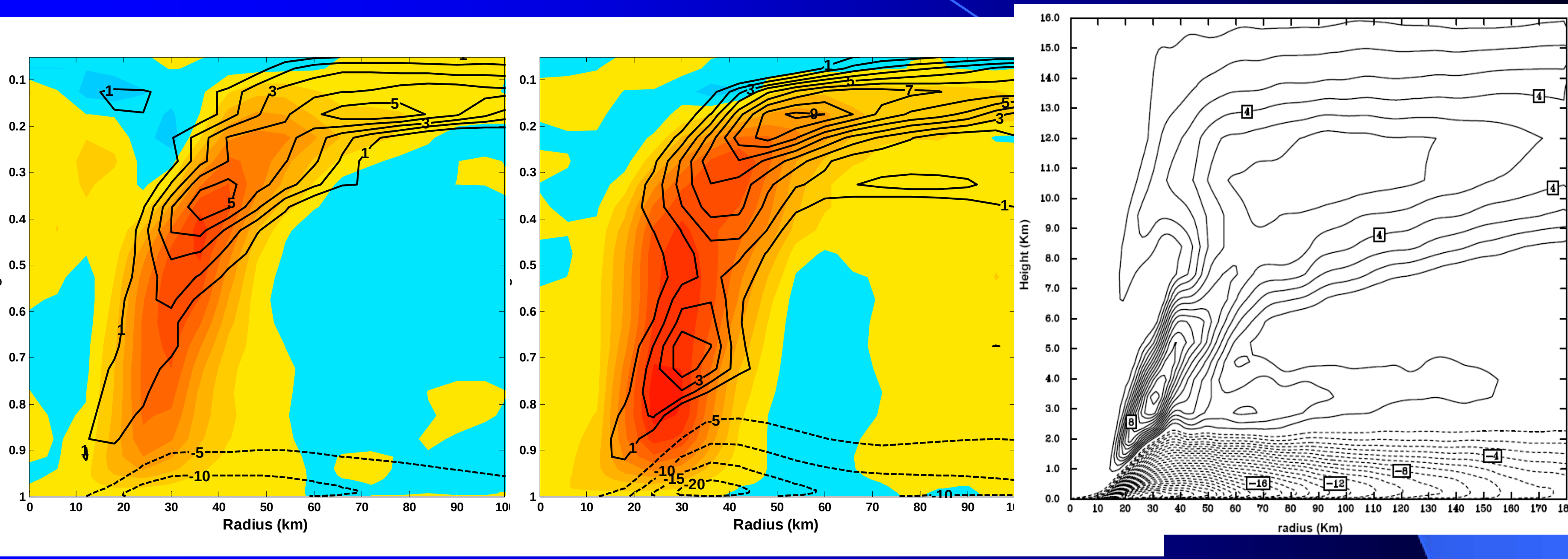

No Terrain

(c.t. = 5 m/s)

50 % Terrain

(c.t. = 5 m/s)

Full Terrain

(c.t. = 1 m/s)

Radial Momentum Budget

- Following Zhang et al. (2001), the governing equation for the radial momentum can be written as

$$\frac{dU}{dt} = -\frac{1}{\rho}\frac{\partial p}{\partial r} + \frac{V^2}{r} + fV - 2\Omega\cos\phi W\cos\lambda + U_D$$

- where

$$\frac{d}{dt} = \frac{\delta}{\delta t} + U'\frac{\partial}{\partial r} + \frac{V'}{r}\frac{\partial}{\partial \lambda} + W\frac{\partial}{\partial z}$$

- and *W*, *U*, and *V* are the vertical, radial and tangential winds; *U'* and *V'* are the horizontal wind components relative to the storm.

Axisymmetric Radial Momentum Budget 9 h before Landfall

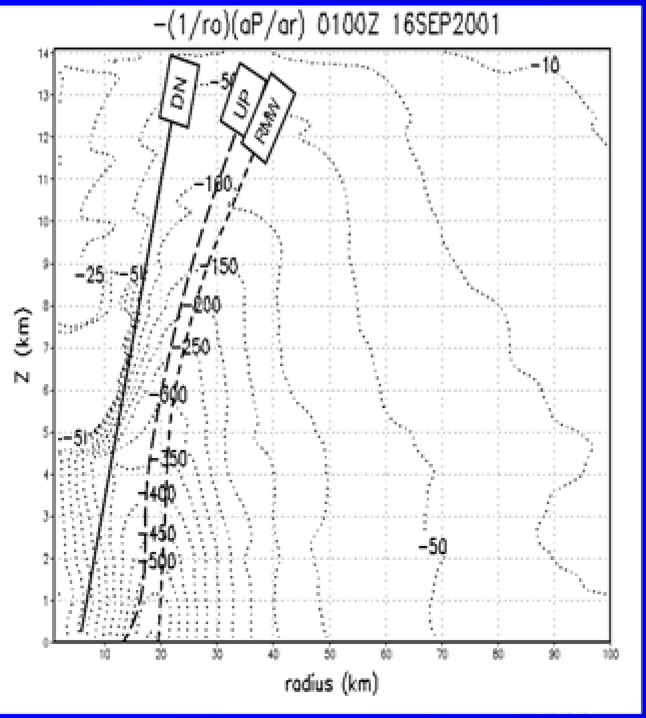

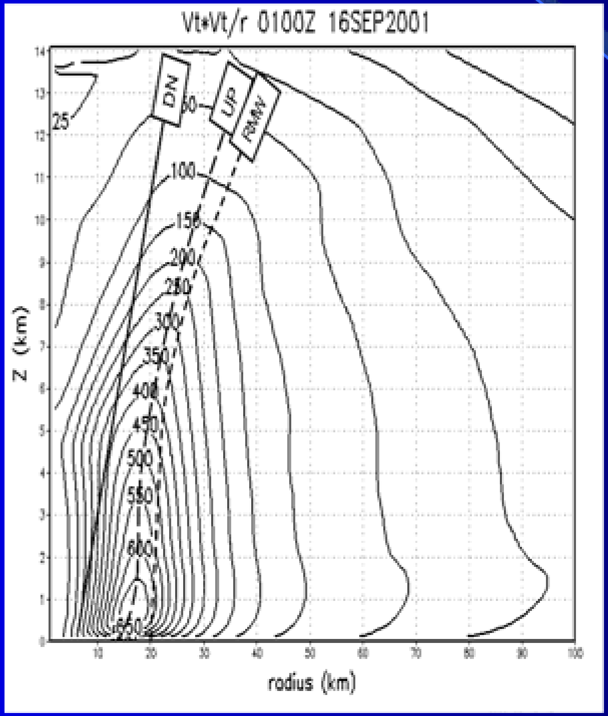

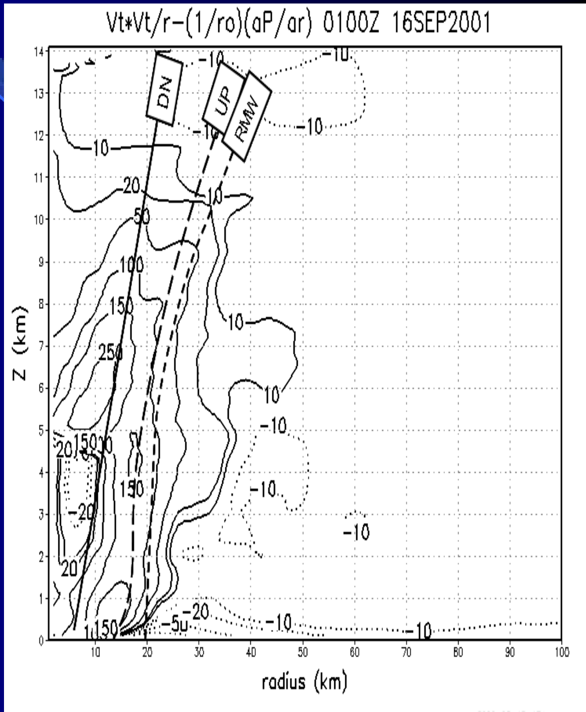

PGF_R (U_P)

Centrifugal force (U_E)

Cyclostrphic force imbalance ($U_P + U_E$)

Oceanic Stage @ 13-14 h

Axisymmetric Radial Momentum Budget
9 h before Landfall

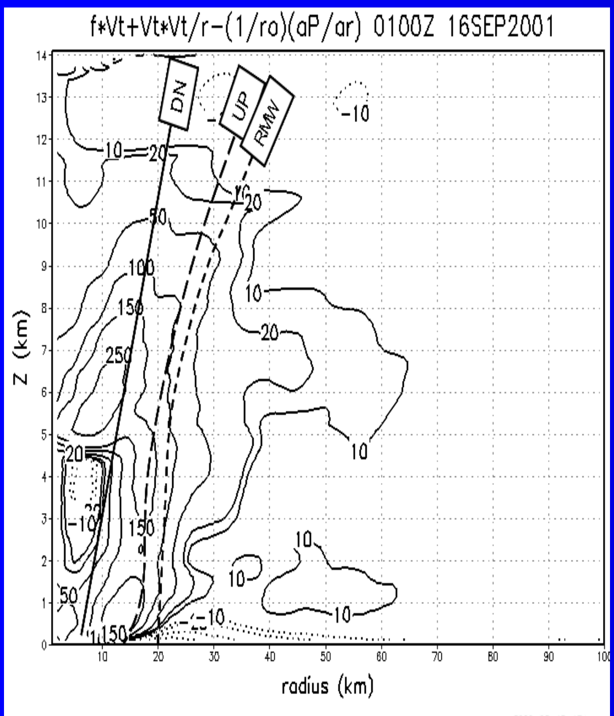

Gradient force imbalance ($U_P + U_E + U_C$)

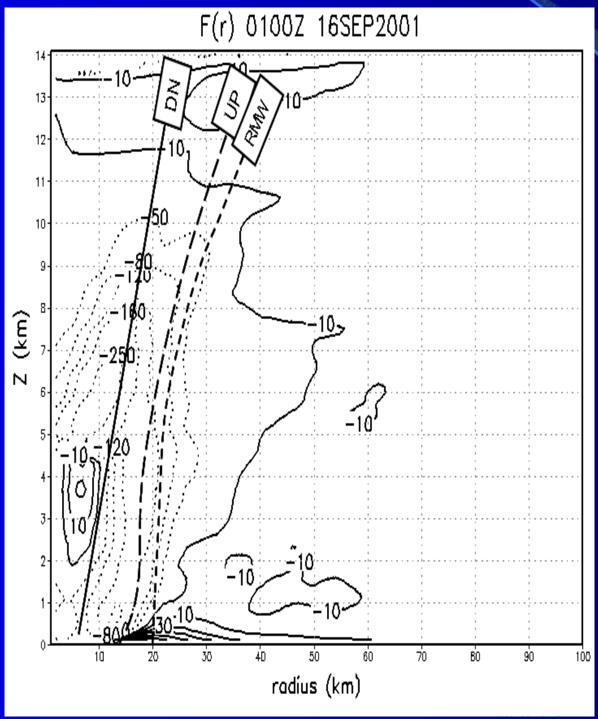

Diffusion & MBL (U_B)

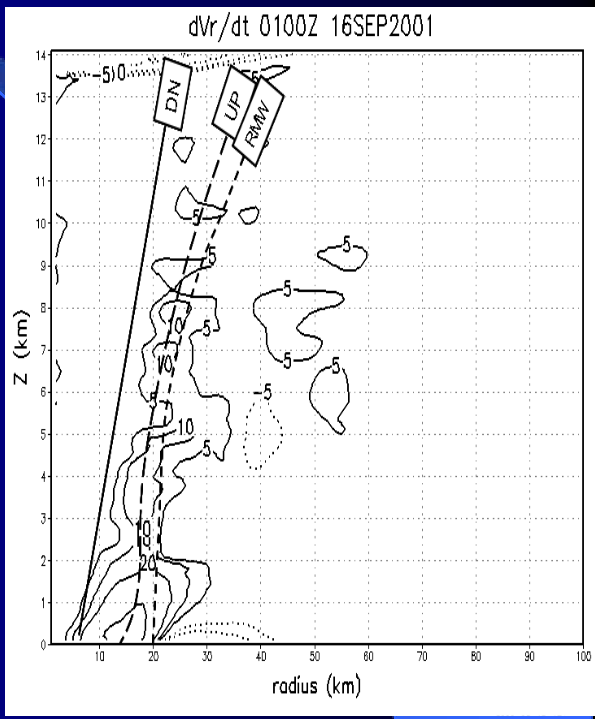

Net Lagrangian tendency (dU/dt)

Oceanic Stage @ 13-14 h

Axisymmetric Radial Momentum Budget 1 h after Landfall

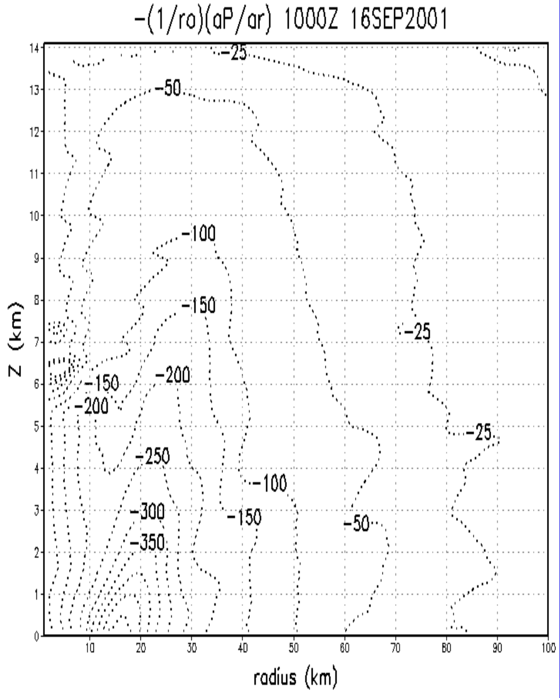

PGF$_R$ (U_P)

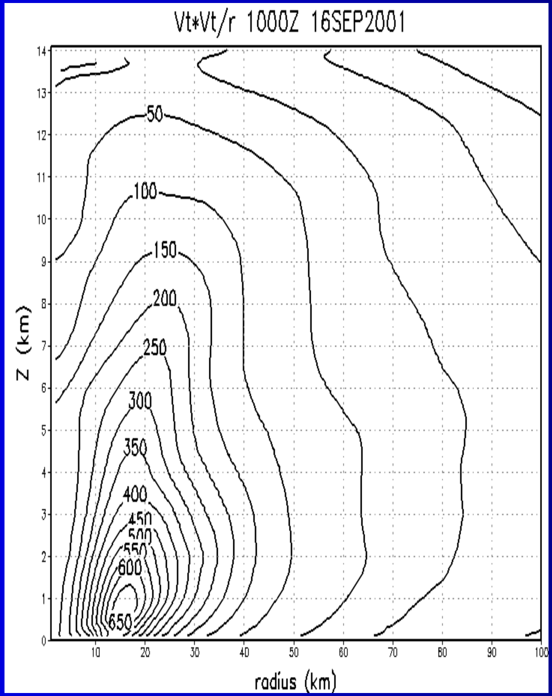

Centrifugal force (U_E)

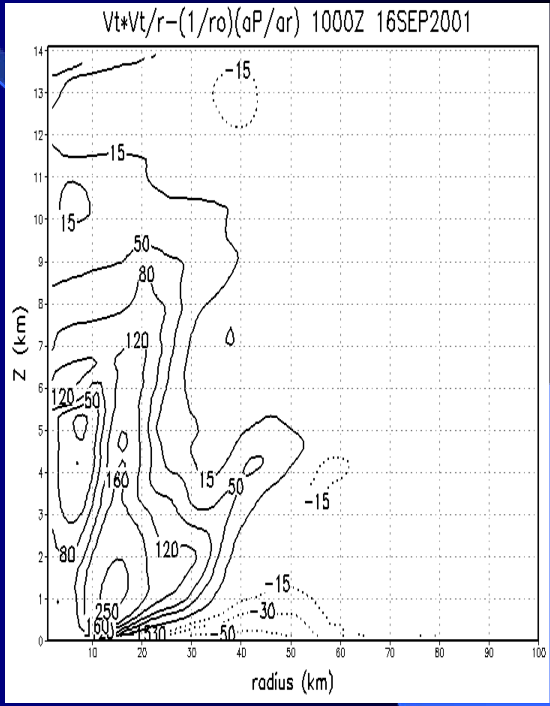

Cyclostrphic force imbalance (U_P + U_E)

Landfall Stage @ 22-23 h

Axisymmetric Radial Momentum Budget 1 h after Landfall

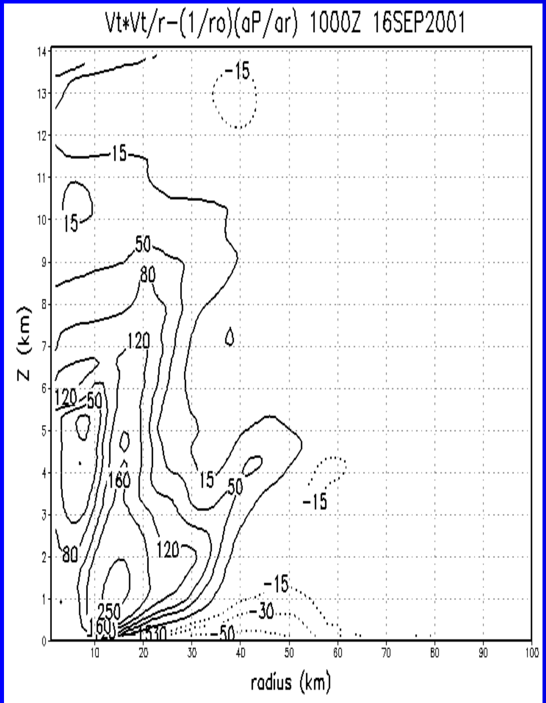

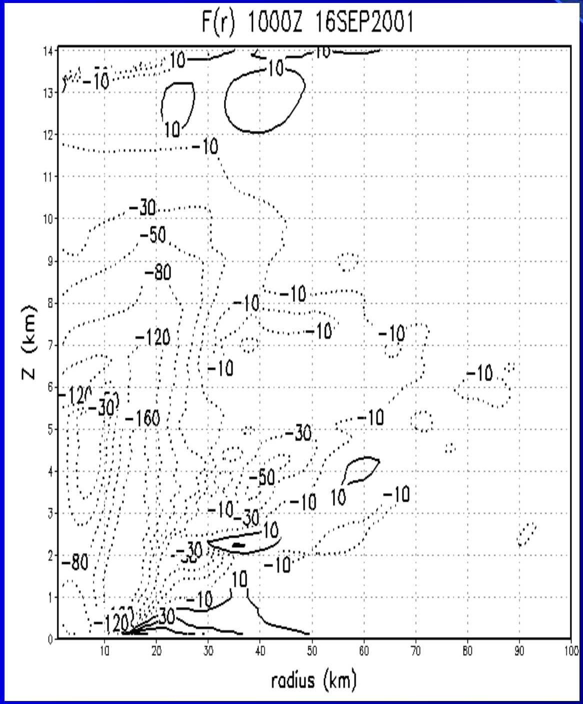

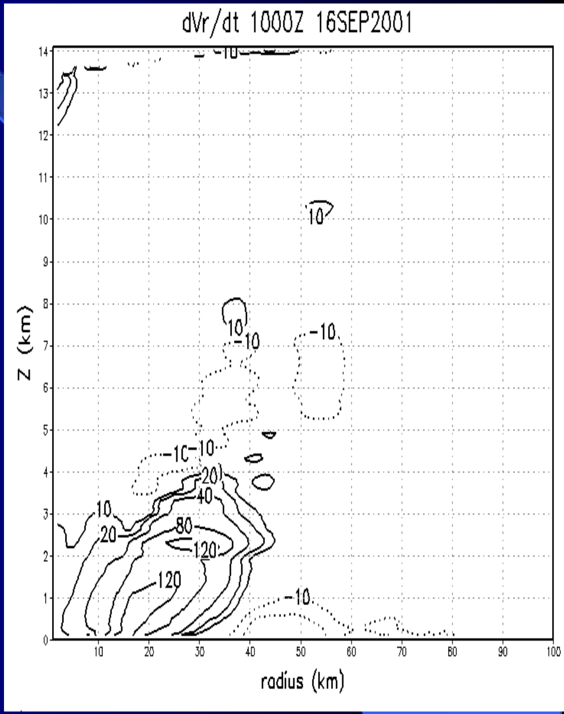

Gradient force imbalance ($U_P + U_E + U_C$)

Diffusion & MBL (U_B)

Net Lagrangian tendency (dU/dt)

Landfall Stage @ 22-23 h

Axisymmetric Radial Momentum Budget 1 h after Landfall

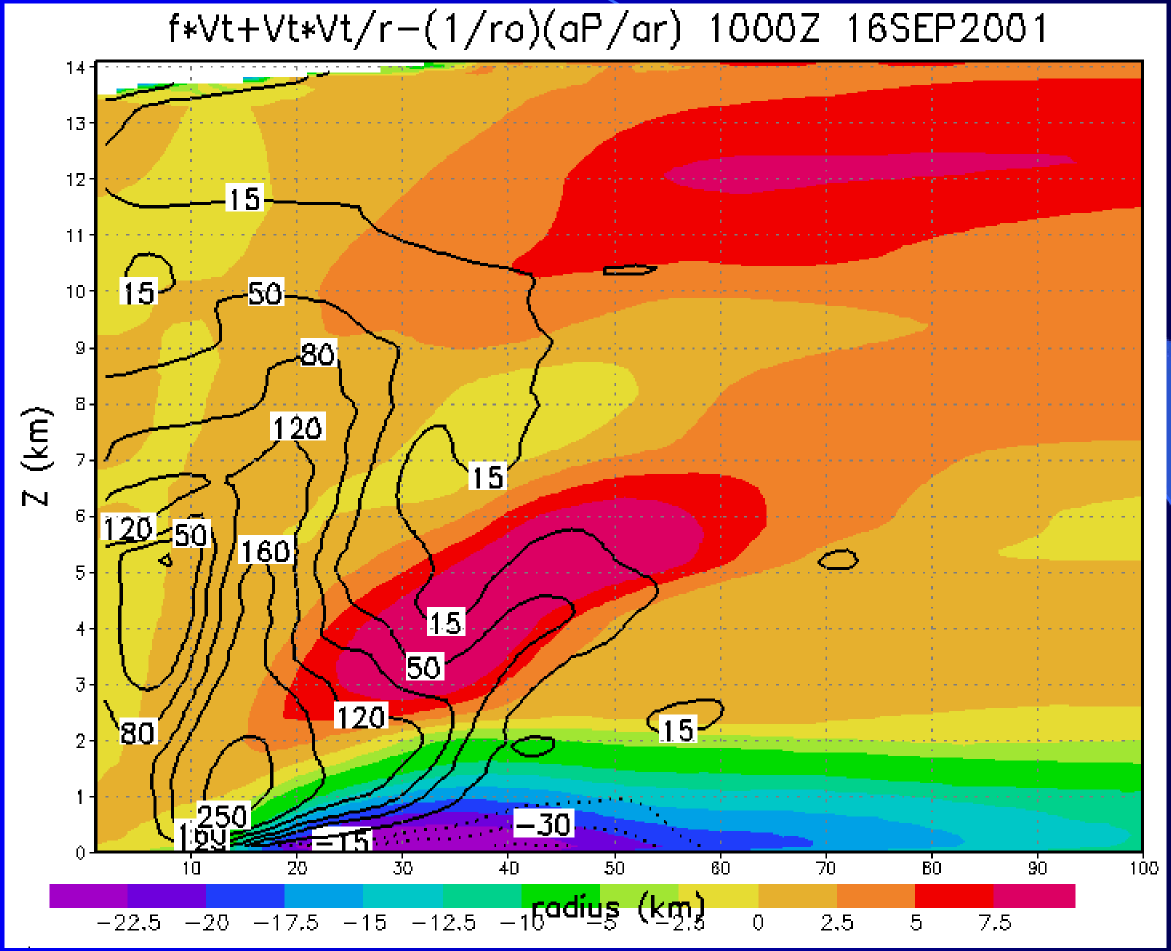

Contour: Gradient force imbalance

Color: Radial flow (U')

Landfall Stage @ 22-23 h

Horizontal Cross Sections of Vertical Velocity (colored) & Radial Wind (contoured)

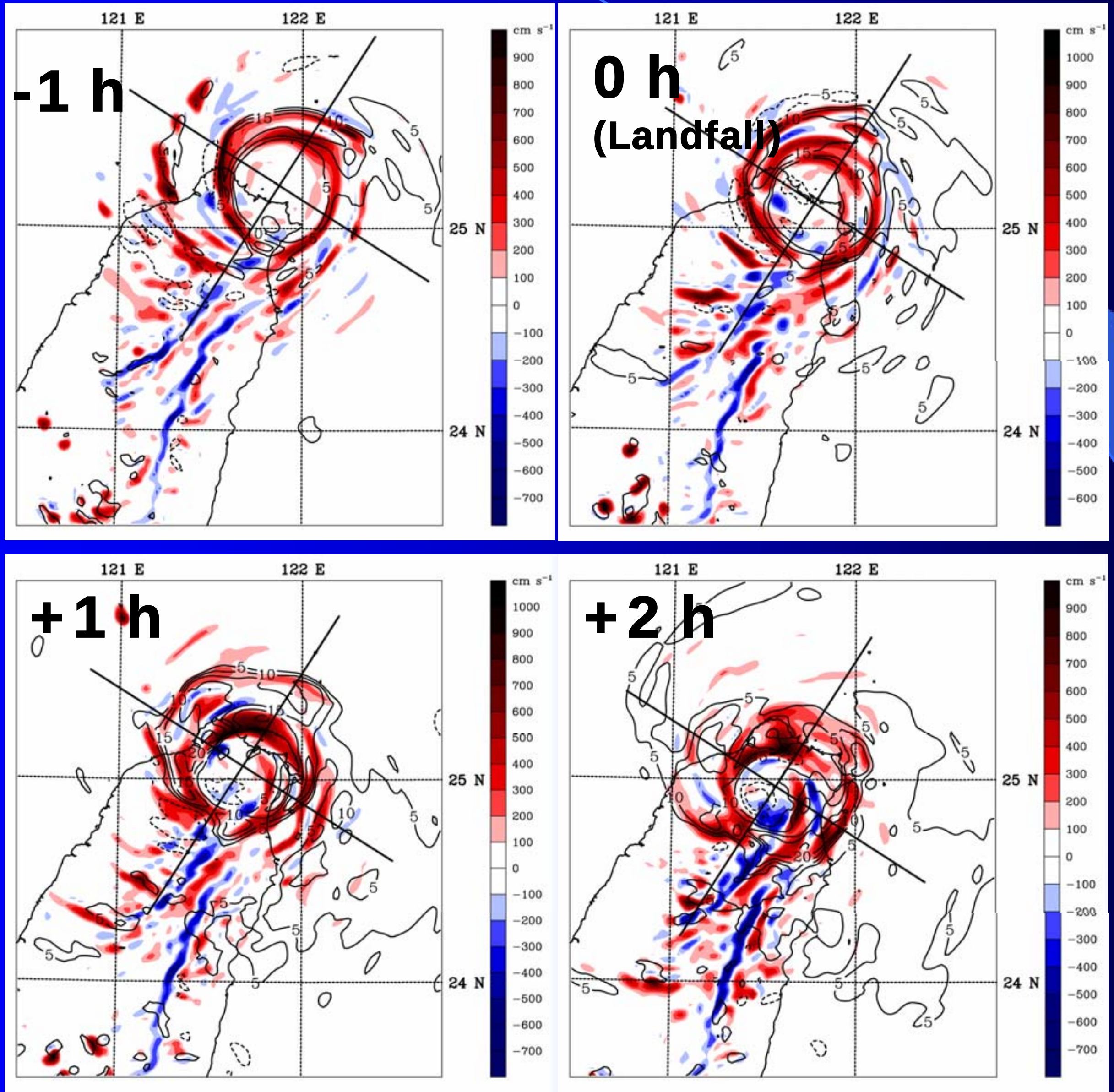

SW-NE Vertical Cross Sections of Vertical Velocity (colored) & Radial Wind (contoured)

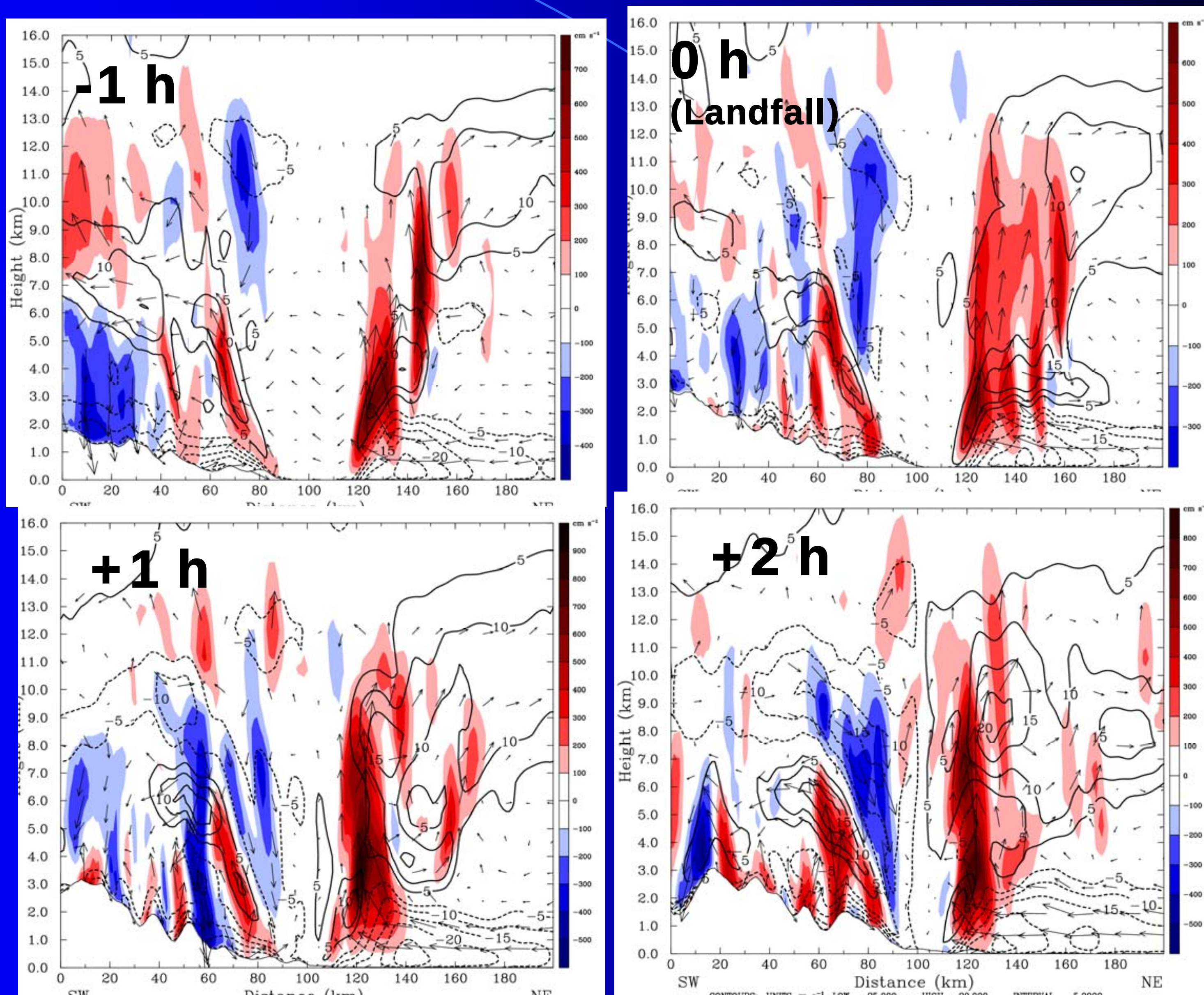

Conclusions (I)

- Precipitation structure changes after landfall:

→Precipitation is widely spread over a larger area.

→Cloud water amount averaged within the inner core is nearly doubled and maximized at lower level.

→Rain water amount averaged within the inner core is increased by 50-70%, mainly produced by melting by graupel particles.

→Ice-phase hydrometeors remain similar vertical profiles after landfall.

- The dominant latent heating (cooling) process within the inner core is condensational heating (evaporative cooling); ice-phase processes are more important in outer rainbands.

Conclusions (II)

- Latent-heating/cooling structure changes:

→Condensational heating avg. within inner core is almost doubled, and maximized at lower height

→Evaporative cooling avg. within inner core is increased by 50-70%

→Total latent heating within inner core is stronger (almost doubled for peak intensity) and located at a lower height (5 km to 3.5 km) after landfall

- After Nari's landfall on Taiwan, the axis of RMW is tilted outward. Tangential wind is reduced by the enhanced surface friction and turbulence mixing over topography.

Conclusions (III)

- After Nari's landfall, the radial inflow at low level becomes stronger and thicker, and strong updrafts occur within the eye, due to enhanced convergence over terrain.

- The centrifugal force (U_E) is greater than the pressure gradient and Coriolis forces ($U_P + U_C$), leading to supergradient winds over Taiwan's topography. It results in the sloping radial outflow jet at middle level over the terrain.

- After landfall, Taiwan topography imposes significant asymmetries on the radial acceleration terms, resulting in strong asymmetries in radial winds.